Journal of African Earth Sciences 129 (2017) 260–281

Contents lists available at ScienceDirect

Journal of African Earth Sciences

journal homepage: www.elsevier.com/locate/jafrearsci

Sedimentology and paleoenvironments of a new fossiliferous late Miocene-Pliocene sedimentary succession in the Rukwa Rift Basin, Tanzania

Cassy Mtelela [a, b, *], Eric M. Roberts [a], Hannah L. Hilbert-Wolf [a], Robert Downie [c], Marc S. Hendrix [d], Patrick M. O'Connor [e, f], Nancy J. Stevens [e, f]

[a] Department of Geosciences, College of Science and Engineering, James Cook University, Townsville, QLD 4811, Australia
[b] Department of Geology, University of Dar es Salaam, P.O. Box 35052, Dar es Salaam, Tanzania
[c] Heritage Oil Ltd, 5 Hanover Square, London W1S 1HQ, UK
[d] Department of Geosciences, University of Montana, Missoula, MT 59812, USA
[e] Department of Biomedical Sciences, Heritage College of Osteopathic Medicine, Ohio University, Athens, OH 45701, USA
[f] Ohio Center for Ecology and Evolutionary Studies, Ohio University, Athens, OH 45701, USA

ARTICLE INFO

Article history:
Received 7 July 2016
Received in revised form
5 January 2017
Accepted 6 January 2017
Available online 11 January 2017

Keywords:
Sedimentology
Neogene
Rukwa
Tanzania
Facies

ABSTRACT

This paper presents a detailed sedimentologic investigation of a newly identified, fossiliferous Late Neogene sedimentary succession in the Rukwa Rift Basin, southwestern Tanzania. This synrift deposit is a rare and significant new example of a fossiliferous succession of this age in the Western Branch of East Africa Rift System. The unit, informally termed the lower Lake Beds succession, is late Miocene to Pliocene in age based on cross-cutting relationships, preliminary biostratigraphy, and U-Pb geochronology. An angular unconformity separates the lower Lake Beds from underlying Cretaceous and Oligocene strata. Deposition was controlled by rapid generation of accommodation space and increased sediment supply associated with late Cenozoic tectonic reactivation of the Rukwa Rift and synchronous initiation of the Rungwe Volcanic Centre. The lower Lake Beds, which have thus far only been identified in three localities throughout the Rukwa Rift Basin, are characterized by two discrete lithologic members (herein A and B). The lower Member A is a volcanic-rich succession composed mostly of devitrified volcanic tuffs, and volcaniclastic mudstones and sandstones with minor conglomerates. The upper Member B is a siliciclastic-dominated succession of conglomerates, sandstones, mudstones and minor volcanic tuffs.

Detailed facies analysis of the lower Lake Beds reveals various distinctive depositional environments that can be grouped into three categories: 1) alluvial fan; 2) fluvial channel; and 3) flood basin environments, characterized by volcanoclastic-filled lakes and ponds, abandoned channel-fills and pedogenically modified floodplains. Member A represents a shallow lacustrine setting filled by tuffaceous sediments, which grade up into a system of alluvial fans and high-energy, proximal gravel-bed braided rivers. An unconformity marks the contact between the two members. Member B shows an upward transition from a high-energy, gravel-bed braided river system to a sandy braided river system with increasingly abundant floodplain deposits and well-developed paleosols. Vertebrate fossils are sparse in member A, but common in member B, preserved both within pedogenic soil horizons and as isolated elements and microsites within fluvial channel facies associations. Faunal remains include fishes, turtles and crocodylians, along with well-preserved mammal cranial and post-cranial remains. In addition, freshwater gastropod shells are locally present in member A and continental trace fossils, including abundant fossilized termite nests, are present in both members.

© 2017 Elsevier Ltd. All rights reserved.

1. Introduction

The Cenozoic East African Rift System (EARS) is well-known for its extensive exposures of richly fossiliferous sedimentary deposits

* Corresponding author. Department of Geosciences, College of Science and Engineering, James Cook University, Townsville, QLD 4811, Australia.
E-mail address: cmtelela@udsm.ac.tz (C. Mtelela).

http://dx.doi.org/10.1016/j.jafrearsci.2017.01.010
1464-343X/© 2017 Elsevier Ltd. All rights reserved.

and rift-related volcanism. The distribution of vertebrate fossils, including hominin remains, is known primarily from sedimentary deposits in the Eastern Branch of the EARS (e.g., the Ethiopian, Kenyan and Gregory rifts; Brown and Feibel, 1986; Dunkleman, 1986; Fleagle et al., 1991; Hautot et al., 2000; Feibel, 2011). The most famous Miocene-Pleistocene fossil sites in the EARS include Olduvai Gorge and Laetoli in northern Tanzania, the Omo-Turkana basin along Ethiopia-Kenya border, in addition to the Middle Awash, Gona, Hadar and Konso areas within the southern Afar depression of northwestern Ethiopia (e.g., Leakey and Leakey, 1964; Bishop, 1978; White and Suwa, 1987; Leakey et al., 1995; Haile-Selassie et al., 2015). The other major locations in Africa where fossil assemblages of this age with abundant vertebrate faunas and early hominin remains have been discovered is in the Cradle of Humankind just outside of Johannesburg, South Africa. Here, fossil cave sites such as Sterkfontein, Swartkrans, Kromdraai, Drimolen, Gondolin, Gladysvale, Malapa and Rising Star have produced a wealth of Plio-Pleistocene fossils (Lockwood and Tobias, 1999; Menter et al., 1999; Susman and de Ruiter, 2004; Pickering et al., 2007; Berger et al., 2010, 2015; Berger, 2012; Herries and Adams, 2013; Dirks et al., 2010, 2015).

The search for fossiliferous strata documenting this important time interval reaches beyond just South Africa and the Eastern Branch of the EARS, as demonstrated by fossil discoveries in the Lake Chad Basin of Central Africa that extend the record of human evolution back to ~7 Ma ago (Brunet et al., 2002, 2005). However, despite decades of paleontologic exploration, only a handful of fossiliferous Miocene-Pleistocene sedimentary deposits have been documented from the Western Branch (Albertine Rift) of the EARS (Pickford et al., 1993; Bromage et al., 1995a,b; Crevecoeur et al., 2014). These rare Western Branch sites are largely limited to the northern part of the rift branch between Lake Albert and Lake Edward, where lower Miocene to Pleistocene deposits have been described from both the DRC and Uganda. In particular, the Semliki Valley to the south of Lake Albert in Uganda (Pickford et al., 1993), and Ishango on the north side of Lake Edwards (Crevecoeur et al., 2014), have both produced abundant faunal remains which together form part of a fairly extensive succession of fossiliferous lower Miocene-Pleistocene fluvio-lacustrine strata in this region (Roller et al., 2010). To date, the only significant fossil locality of this age in the southern portion of the EARS is in the northern Malawi Rift Basin, a segment of the Western Branch of the East African Rift System (Betzler and Ring, 1995; Roller et al., 2010). The Uraha, Mwenirondo, Malema and Mwimbi sites on the northwestern shores of Lake Malawi preserve a number of relatively isolated, fossiliferous, fluvio-lacustrine, Plio-Pleistocene deposits defined as the Chiwondo beds, which have produced abundant faunal remains, along with a single hominin dentary and other isolated jaw fragments (Clark et al., 1970; Bromage et al., 1985, 1995a, b; Rozzi et al., 1997; Sandrock et al., 2007; Kullmer et al., 2011; Stewart and Murray, 2013).

The late Cenozoic, between 10 Ma and Recent, represents a critical time period in African history, characterized by major environmental and climatic changes associated with the development of the East African Rift System and uplift of southern and eastern Africa (Potts, 1998; deMenocal, 2004; Sepulchre et al., 2006; Maslin and Christensen, 2007; Trauth et al., 2007). It has been suggested that tectonic rifting has played an important role in faunal evolution in Africa, particularly by creating diverse landscapes with dispersal corridors and settings conducive to the development of major river systems and lakes where a mosaic of African species are thought to have lived and evolved (Brown, 1981; Feibel et al., 1991; Potts, 1998; Ashley, 2000; Trauth et al., 2007). Additionally, tectonic rifting is associated with volcanism and high subsidence rates that provide excellent conditions for the production and deposition of sediments, and hence rapid burial of floral and faunal remains (WoldeGabriel et al., 2000; Stollhofen et al., 2008). Rift basins are therefore, important archives of high-resolution tectonic, climatic and environmental data.

Nowhere has the importance of such changes in Africa been of more interest than in the study of the East African Rift System, which has long focused on the interplay between tectonic, environmental and climatic changes for understanding the evolutionary and ecological patterns and distribution of flora and fauna on the continent since the late Miocene (e.g., Vrba, 1988; deMenocal, 1995; Stanley, 1995; Potts, 1998; Kingston, 2007; Maslin and Christensen, 2007; Trauth et al., 2007; Maslin et al., 2014). A key aspect of expanding our understanding of the evolution of East African landscapes and ecosystems depends upon recognition and discovery of new outcrop exposures, particularly in previously under-studied or unknown basins. Whereas late Neogene deposits in the Eastern Branch of the East African Rift System have been extensively explored and studied, many parts of the Western Branch of the EARS have yet to be extensively explored and documented. In this paper, we document a vertebrate, invertebrate and trace fossil-bearing late Neogene stratigraphic succession in the Rukwa Rift Basin of southwestern Tanzania, informally referred to here as the lower Lake Beds succession. This study was conducted as part of the Rukwa Rift Basin Project (see Roberts et al., 2004, 2010, 2012; O'Connor et al., 2006, 2010; Stevens et al., 2008, 2013), which is focused on the discovery and documentation of the palaeontologic history of the rift over the last 100 million years in combination with refining the tectonic and sedimentary history of the basin. The purpose of this paper is to describe the distribution and detailed sedimentology of the lower Lake Beds Succession and to provide a preliminary stratigraphic and paleoenvironmental context for this newly recognized Neogene vertebrate fossil locality in East Africa.

2. Regional geology and background

The northwest-trending Rukwa Rift Basin (RRB) is part of the Western Branch of the East African Rift System, situated between the Tanganyika and Malawi rifts in southwestern Tanzania (Fig. 1). The basin is about 360 km long and 40 km wide, bounded to the northeast by the linear Lupa border fault and Tanzania Craton, to the southwest by the Ufipa fault and uplifted Ufipa block, and to the south and southwest by the Rungwe volcanics and Mbozi block, respectively (Ebinger et al., 1989; Kilembe and Rosendahl, 1992). The RRB has a half-graben architecture, and is flanked by uplifted Paleoproterozoic metamorphic basement rocks of the Ubendian shear belt (Quennell et al., 1956; Daly et al., 1985; Lawley et al., 2013).

The Rukwa Rift was initiated during the Paleozoic by reactivation of Paleoproterozoic to Neoproterozoic sinistral shear zones in the NW-SE trending Ubendian Belt (Theunissen et al., 1996). Structural development of the RRB has provoked debate among researchers. The RRB was first proposed to have formed as a strike-slip pull-apart basin in an oblique, northwest-southeast extensional setting based on interpretations of linear map geometry and oblique orientation to the general north-south trend of EARS, as well as from satellite images and seismic profiles (Chorowicz and Mukonki, 1980; Kazmin, 1980; Tiercelin et al., 1988). The oblique opening model was later supported by outcrop-based structural studies that indicated dominantly low angle, dextral kinematics along the Lupa Fault (Wheeler and Karson, 1994). However the basin geometry and listric fault shape observed in seismic reflection data does not fit a pull-apart basin, and other workers have suggested east-west to northeast-southwest extension, and oblique opening of an extensional rift basin, influenced by northwest-

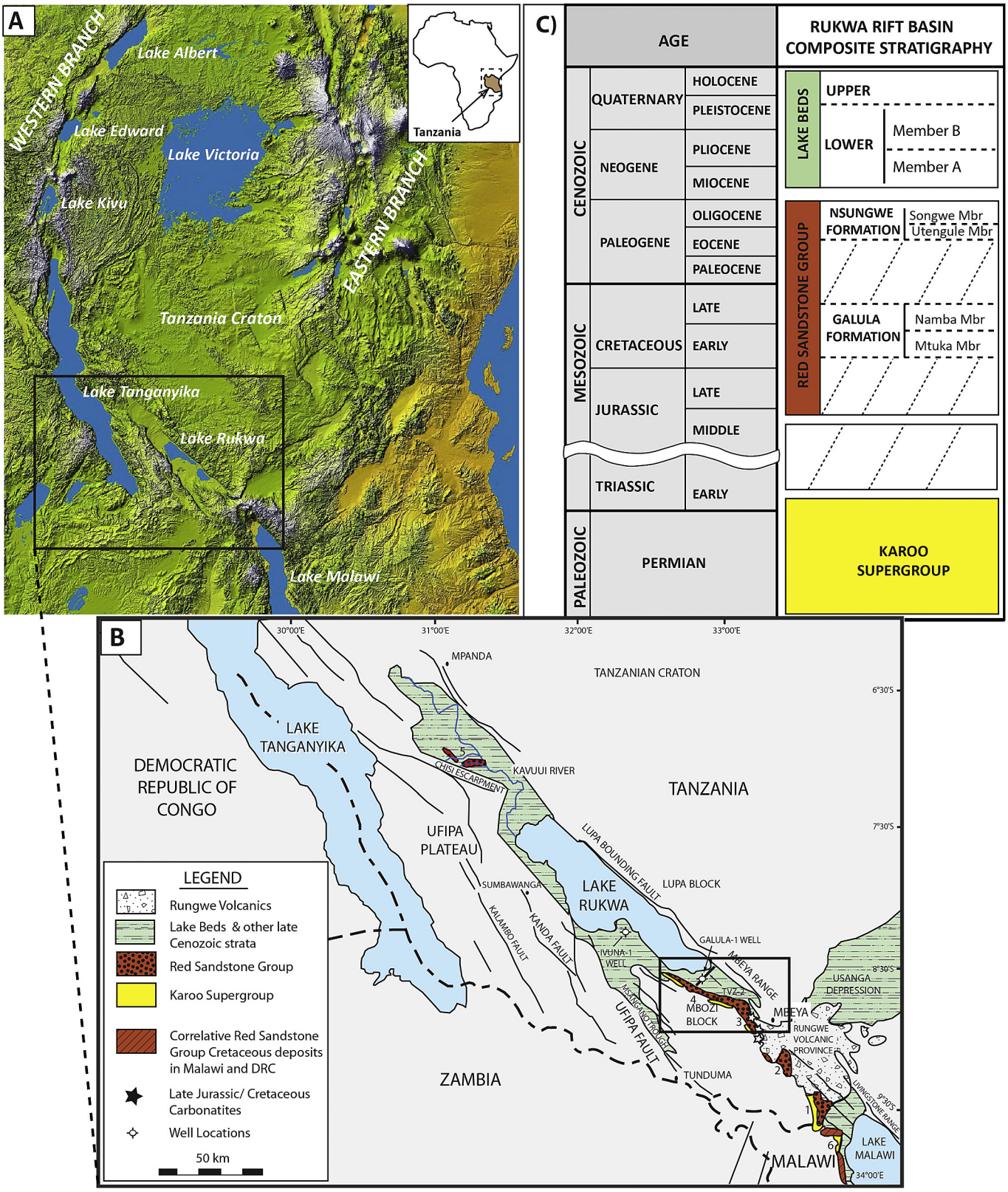


Fig. 1. **A)** Map showing study area in southwestern Tanzania. **B)** Geological map of the Rukwa Rift Basin showing tectonic elements and distribution of rock units. Inset box is shown in Fig. 2A. **C)** Composite stratigraphy of the Rukwa Rift Basin (modified from Roberts et al., 2010).

southeast trending pre-existing fabric in the basement (Ebinger, 1989; Morley et al., 1992; Mbede, 1993). Thus, a general E-W extension model was proposed, dominated by normal faulting sub-orthogonal to the trends of the rift segments (orthogonal opening model: Ebinger, 1989; Morley et al., 1992; Delvaux, 2001; Delvaux and Barth, 2010; Morley, 2010).

The orthogonal opening model for the Rukwa Rift Basin is supported by more recent work on the ancient and active faults along the Ufipa Plateau. Based on detailed active tectonic studies, brittle kinematics and paleostress investigations, Delvaux et al. (2012) has shown that extension occurred sub-orthogonal to the NW-SE rift trend in a normal faulting regime. These workers hypothesized the existence of two brittle regimes that pre-date the late Neogene development of the East African Rift System. According to Delvaux et al. (2012), the oldest brittle regime initiated sometime prior to the late Carboniferous, and is characterized by eastward thrusting with compression sub-orthogonal to the trend of the Ubende Belt and subsequent rift segmentation. This deformation episode was associated with the interaction between Bangweulu Block and the Tanzanian Craton during the late stages of the Pan-African orogeny (Ebinger, 1989; Morley et al., 1992; Delvaux et al., 2012). The youngest brittle stage, which is characterized by N-S transpression and related dextral fault movements, is linked to Mesozoic far-field stresses associated with rifting along the southern passive margin of Gondwana (Delvaux et al., 2012).

Seismic and gravity surveys conducted in the RRB during 1980s and 1990s, along with the drilling of two hydrocarbon exploration wells (Galula-1 and Ivuna-1 drilled in 1987), revealed up to 8–11 km of sedimentary fill in the basin, making it one of the thickest continental sedimentary basins in Africa (see Figs. 8–11 in Morley et al., 1999). Analysis of the seismic profiles coupled with well data and surface geology show that the RRB has undergone at least four episodes of rifting, including: (1) a Permo-Triassic event, which resulted in the deposition of Karoo Supergroup equivalent strata (Kilembe and Rosendahl, 1992; Morley et al., 1999); (2) a Cretaceous rifting event that deposited the fluviatile Galula Formation, a unit that is subdivided into two distinct members (lower part of the Red Sandstone Group: Roberts et al., 2004, 2010, 2012); (3) a late Oligocene event that resulted in a short-lived, richly fossiliferous fluvio-lacustrine depositional sequence (Nsungwe Formation, upper part of the Red Sandstone Group), which was accompanied by alkaline volcanism (Roberts et al., 2004, 2010, 2012); and (4) late Miocene to Recent rifting and deposition of the Lake Beds succession, accompanied by voluminous bimodal volcanism in the Rungwe Volcanic Province (Grantham et al., 1958; Ebinger et al., 1989; Wescott et al., 1991).

The Lake Beds succession, which represents the youngest stratigraphic interval in the RRB, is widespread and relatively thick, reaching up to 4 km (see Kilembe and Rosendahl, 1992). In the southern RRB, Lake Beds deposits are well exposed in the Ilasilo-Galula, Ikuha and Ikumbi areas, as well as in the Songwe Valley and along the Chambua, Hamposia, Namba and Chizi river drainages (Fig. 2A). The Lake Beds deposits unconformably overlie the late Oligocene Nsungwe Formation or the Cretaceous Galula Formation of the Red Sandstone Group (Roberts et al., 2010). The Lake Beds units were first described by Grantham et al. (1958) as conglomerates, sandstones and mudrocks associated with fluvial-floodplain and lacustrine environments. Grantham et al. (1958) informally subdivided the Lake Beds into lower and upper units, based on structural and lithological features. According to Grantham et al. (1958), the lower (older) unit consists of gently NE-dipping sandstone and overlying volcanic siltstone, whereas the upper (younger) unit is characterized by flat-lying beds of conglomerate, pumice tuff and limestone. Earlier efforts to determine the depositional age of the Lake Beds involved contentious microfloral analysis of the Ivuna-1 and Galula-1 well cuttings, which suggested a late Pliocene-Holocene age for the large portion of the Lake Beds (e.g., Wescott et al., 1991). Radiocarbon dating of shallow (12.8 m thick) sediment cores suggested a Quaternary age for this uppermost interval of the strata (e.g., Haberyan, 1987).

Unfortunately, however, there remains no formal stratigraphy for the Lake Beds. To date, the exposed Lake Beds deposits documented by various research teams in the Rukwa Rift have been restricted to the latest Quaternary portion, which is largely devoid of vertebrate fossils except isolated fish elements (Sherwood and Kingston, 2002; Cohen et al., 2013). Over the last few decades, the Lake Beds have also been the focus of brief and unsuccessful exploration focused on identifying new hominin-bearing deposits in this part of the East African Rift System (e.g., Sherwood and Kingston, 2002).

More recently, detailed sedimentologic, geochronologic and biostratigraphic investigations of the uppermost units of the Lake Beds succession have been performed (Cohen et al., 2013; Mtelela et al., 2016). These investigations have largely confirmed a latest Pleistocene-Holocene age between 45 and 5 Ka for all known exposures of the Lake Beds strata in both the northern and southern outcrop extents across the basin (Mtelela et al., 2016). Indeed, sedimentologic investigations conducted by Mtelela et al. (2016) reveal that the “upper” and “lower” Lake Beds as defined and mapped by Grantham et al. (1958) does not represent a true lithostratigraphic subdivision. Rather, these stratigraphic interpretations represent lateral facies changes (sub-environments) within a widely variable fluvial-lacustrine deposition system, and the term upper Lake Beds Succession has been suggested for all of these strata (Mtelela et al., 2016).

However, interpretations of 2-D seismic data across the basin shows that the Lake Beds succession sits above slightly incised and deformed beds of the Red Sandstone Group in a half-graben basin (Kilembe and Rosendahl, 1992; Morley et al., 1999), with bedsets gently dipping and fanning towards the main bounding fault in a north-to-northwest direction. As such, the western rift margin represents a likely site for containing exposures of the basal portion of the Lake Beds stratigraphy, particularly considering the present day low surface level of Lake Rukwa. Indeed, during the course of the recent sedimentological and paleontological investigations of the upper Lake Beds, conducted as part of the Rukwa Rift Basin Project, our research group identified a series of new and previously unrecognized sedimentary deposits cropping out between the Red Sandstone Group and upper Lake Beds deposits in isolated areas within the rift. It appears that recent rifting and uplift have exposed older sedimentary units along the western margin of the basin, in the Songwe Valley (south of the lake) and along the Hamposia, Chizi and Ikumbi River drainages. These strata are termed here the lower Lake Beds (LLB). Perhaps due to the irregular nature of exposures and the blanketing nature of upper Lake Beds strata, exposures of the LLB (described in this paper) were not recognized or mapped during the first regional geologic mapping by Grantham et al. (1958). The total outcrop extent of this unit is unknown and awaits further exploration. The LLB deposits have been folded and faulted along with the Red Sandstone Group strata, clearly differentiating them from the undeformed, horizontally bedded upper Lake Beds strata (Fig. 2B). The sedimentology and paleontology of the LLB (discussed below) is distinctly different from that of both the Oligocene and Cretaceous Red Sandstone Group deposits and the overlying upper Lake Beds strata. Detailed biostratigraphic assessments, to be presented elsewhere (N. Stevens, pers. comm.), and geochronologic data (Hilbert-Wolf et al., 2013) indicate a late Miocene to Pliocene age for these deposits.

3. Methods

A GPS set to the Tanzanian datum (Arc, 1960), Jacob’s Staff, laser range finder, and Brunton compass were utilized for mapping and measuring stratigraphic sections along the upper Hamposia, Chizi and Ikumbi Rivers, where deep channel incision has resulted in well-exposed cliff face exposures of the LLB (Fig. 2). Topographic

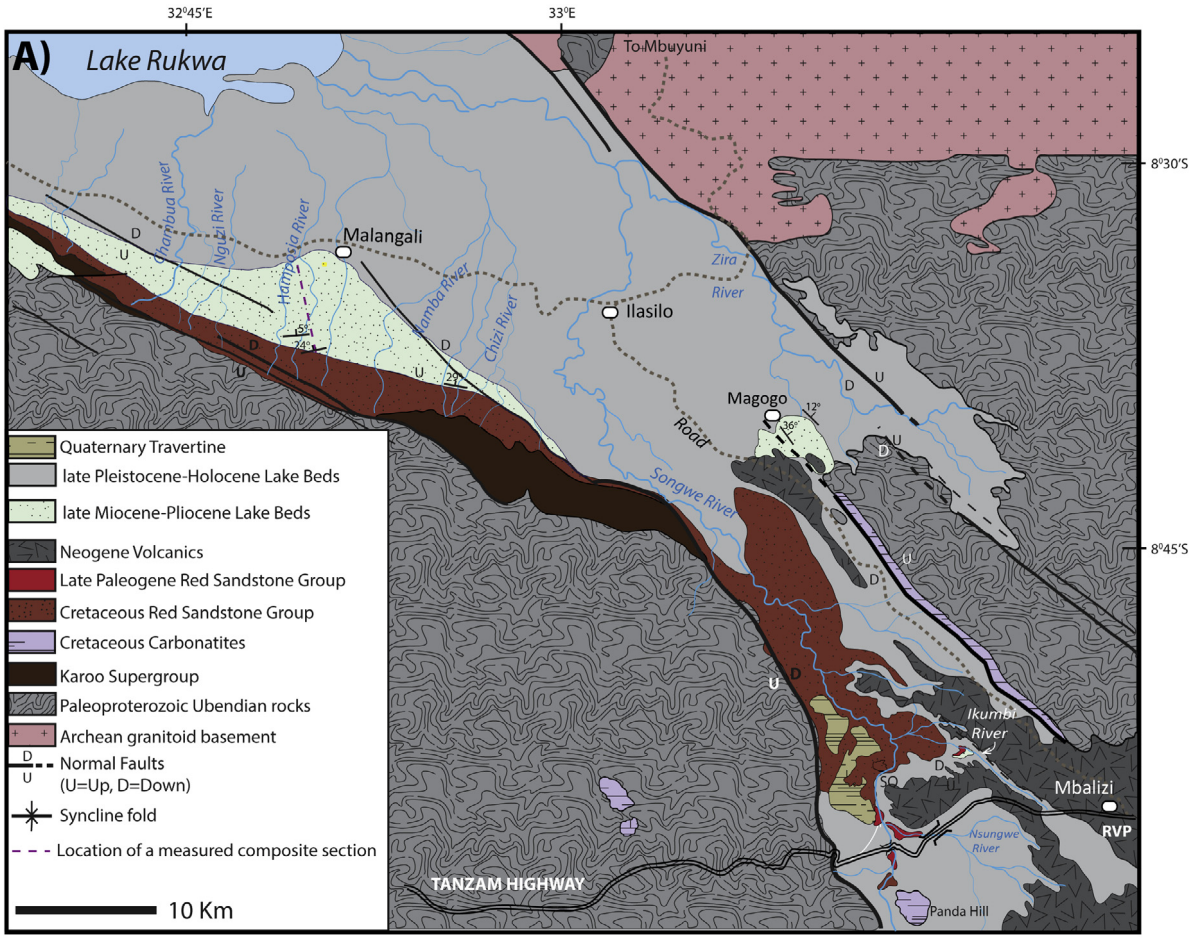




Fig. 2. A) Geologic map of the southern Rukwa Rift Basin, highlighting the distribution of the lower Lake Beds succession along the present-day Chambua, Nguzi, Hamposia, Namba and Chizi river drainages, as well as in the Ikumbi and Magogo areas. Other lithologies and structures are adopted from Grantham et al. (1958) and Roberts et al. (2010). **B)** Unconformable contact between lower Lake Beds and the Cretaceous Red Sandstone Group rocks along the Chizi River. Note that both the Cretaceous and lower Lake Beds strata are dipping in the same direction; however there is a slight angular unconformity that marks the contact between the two units. (For interpretation of the references to colour in this figure legend, the reader is referred to the web version of this article.)

maps and the Mbeya 244 quarter-degree geologic map (Grantham et al., 1958) were used as base maps. A Munsell rock colour chart was used to determine rock colour codes. A Brunton compass was also used to measure bedding trends and palaeocurrent orientations on three-dimensionally exposed ripple, planar and trough cross-stratified beds. Lithofacies were identified and documented based on key sedimentologic aspects, including: lithology, texture (grain-size, shape and sorting), sedimentary and biogenic structures, and fossil content.

Facies analysis was conducted for the lower Lake Beds following the methodology outlined by Mtelela et al. (2016) for the upper Lake Beds. Lithofacies nomenclature and codes used in this study are modified after Miall (1996), to illuminate the distinctive characteristics of the Lake Beds. In particular, we use the terms *tuffaceous conglomerate*, *tuffaceous sandstone* and *bentonitic mudstone* (and their respective codes) for secondary, reworked pyroclastic sedimentary rocks comprised of dominantly pebble-, sand-, and clay-sized sediments, respectively. Pebble counts were performed in the field on conglomerate beds at different levels in the stratigraphy to characterize lithoclast composition and supplement sandstone petrology. Representative sandstone samples were collected for thin-section analysis. The detrital mineral composition of siliciclastic sandstone in thin sections were statistically analyzed by a point counting technique, following a modified Gazzi-Dickinson method (Ingersoll et al., 1984), to determine percentage proportions of chiefly quartz, feldspar and rock fragments.

4. Lithostratigraphy

A continuous ~156 m thick stratigraphic section was measured along the Hamposia River drainage. The lithostratigraphy presented below is based primarily on observations and data collected along this section. However, correlations can be made with strata observed in the other areas, particularly in the Chizi River drainage (Fig. 2). Along the outcrop belt on the western side of Lake Rukwa, the LLB strata rest unconformably on top of the Cretaceous Galula Formation. The basal contact is clearly exposed in cliff-face exposures along both the Chizi and Hamposia rivers. Along the Hamposia and Chizi Rivers, the LLB unconformably overlies the Galula Formation, and dips roughly 18° and 26° towards the NNW and NE, respectively. Along the Ikumbi River, the LLB overlies the Nsungwe Formation, and dips ~6° towards the ENE. At the Hamposia River section, the contact is located at 8°37′54″S, 32°49′10″E, near the village of Mpona, where the LLB dips 18° to the NW, and the underlying Galula Formation dips 24° NW (note very similar strike orientations). The LLB and the Cretaceous strata appears to have been faulted together following deposition of the LLB, but prior to deposition of the Quaternary-Holocene upper Lake Beds strata, which were deposited horizontally above the dipping Galula Formation and LLB strata. The top of the LLB section along the Hamposia River ends at 8°34′35″S, 32°49′49″E, near the vehicle bridge close to Malangali village. At the Ikumbi Section, and in several places within the Songwe area, the LLB also overlie dipping bedding of the late Oligocene Nsungwe Formation (Roberts et al., 2010, 2012; Spandler et al., 2016). In the Ikumbi section, horizontally-stratified ULB units have erosionally incised into both the LLB and the underlying Nsungwe Formation. In the Magogo area, the LLB is steeply dipping and it is unclear what portion of the LLB stratigraphy is exposed. There is no basal contact with the Red Sandstone Group exposed around Magogo, but a basal carbonate unit does occur there that is not observed elsewhere in the study area.

In the Hamposia river section, distinct lithological variations between the lower and upper portions of the LLB stratigraphy, coupled with the presence of major unconformity surfaces within the LLB, permit the subdivision of the LLB into two informal stratigraphic units: lower Member A and upper Member B (Fig. 3). At present, there is insufficient exposure and regional understanding of the stratigraphy to extend these subdivisions to the LLB strata that crop out in the Magogo area and Songwe Valley (e.g., Ikumbi area). Hence, the informal lithostratigraphy presented here is limited to exposures of the LLB along the southwestern margin of Lake Rukwa. Establishment of a formal stratigraphic subdivision and nomenclature for the entire Lake Beds succession awaits a basin-wide synthesis and integration of outcrop based and subsurface (Ivuna-1 and Galula-1 wells) dating of these units recently reported by Hilbert-Wolf et al. (in press).

4.1. Member A

Informal member A is defined as the dominantly tuffaceous lower portion of the LLB that rests unconformably on the Galula or Nsungwe formations. Along the Hamposia River, member A is ~40 m thick and capped by deeply weathered paleosol horizon that is cut by a high-relief erosional unconformity separating it from the overlying fluvial strata of member B. The basal 23 m of member A is characterized by a distinctive siliciclastic-dominated facies consisting of tabular to lenticular quartz pebble conglomerate, resting unconformably above the Red Sandstone Group. Paleocurrent measurements suggest deposition by NW directed longitudinal fluvial channels. This basal interval is significant in that it also lacks volcanic detritus or pyroclastic units. The middle interval of member A transitions sharply to a volcanic-rich succession of tuff, tuffaceous conglomerate and bentonitic mudstone. The upper-most part of member A transitions back to a more siliciclastic-rich succession of muddy sandstone and conglomerate. However, the matrix and some of the clasts of these upper sandstone and conglomerate units retains a volcanic nature with abundant bentonitic mudstone and devitrified volcanic ash.

Conglomerate units at the bottom and top of member A are vein-quartz dominated. Individual beds are typically characterized by an upward transition from a primarily clast-supported to a matrix-supported towards the top. Siliciclastic sandstone framework grain compositions vary from quartzose to quartzo-feldspathic (subarkosic), and vary in colour between very light gray (N8), pale red (5R 6/2) and grayish orange pink (5YR 7/2). Volcaniclastic lithofacies that dominate the middle of member A are composed of a combination of primary pyroclastic deposits and re-sedimented volcanic-rich sedimentary deposits. The pyroclastic deposits are primarily unwelded, pumice-rich ash flow tuff and ash fall tuff lithofacies. In most cases, the primary volcanic glass is weathered and has devitrified or partially devitrified into smectitic clays. The strike and dip change up-section due to post-depositional faulting, from 82°/18° NNW at the base, to 20°/7° WNW in the upper part of the section through this unit. Fossils recovered from member A are limited to isolated fish bones and fragments of large mammal bones that occur in the beds of siliciclastic sandstone lithofacies towards the upper part of this unit.

4.2. Member B

Informal member B is considerably thicker (~110 m thick in outcrop) than member A, and is defined as the siliciclastic-dominated interval above the unconformity at the top of member A. In the type section along the Hamposia River described in this study, the dip of member B shallows considerably up-section to almost zero. Member B can be followed for ~5–6 km along the Hamposia river drainage, from the Mpona area to the western part of the Malangali village. In many places along this river section, the overlying upper Lake Beds succession erosionally overlies member B with an angular unconformity.

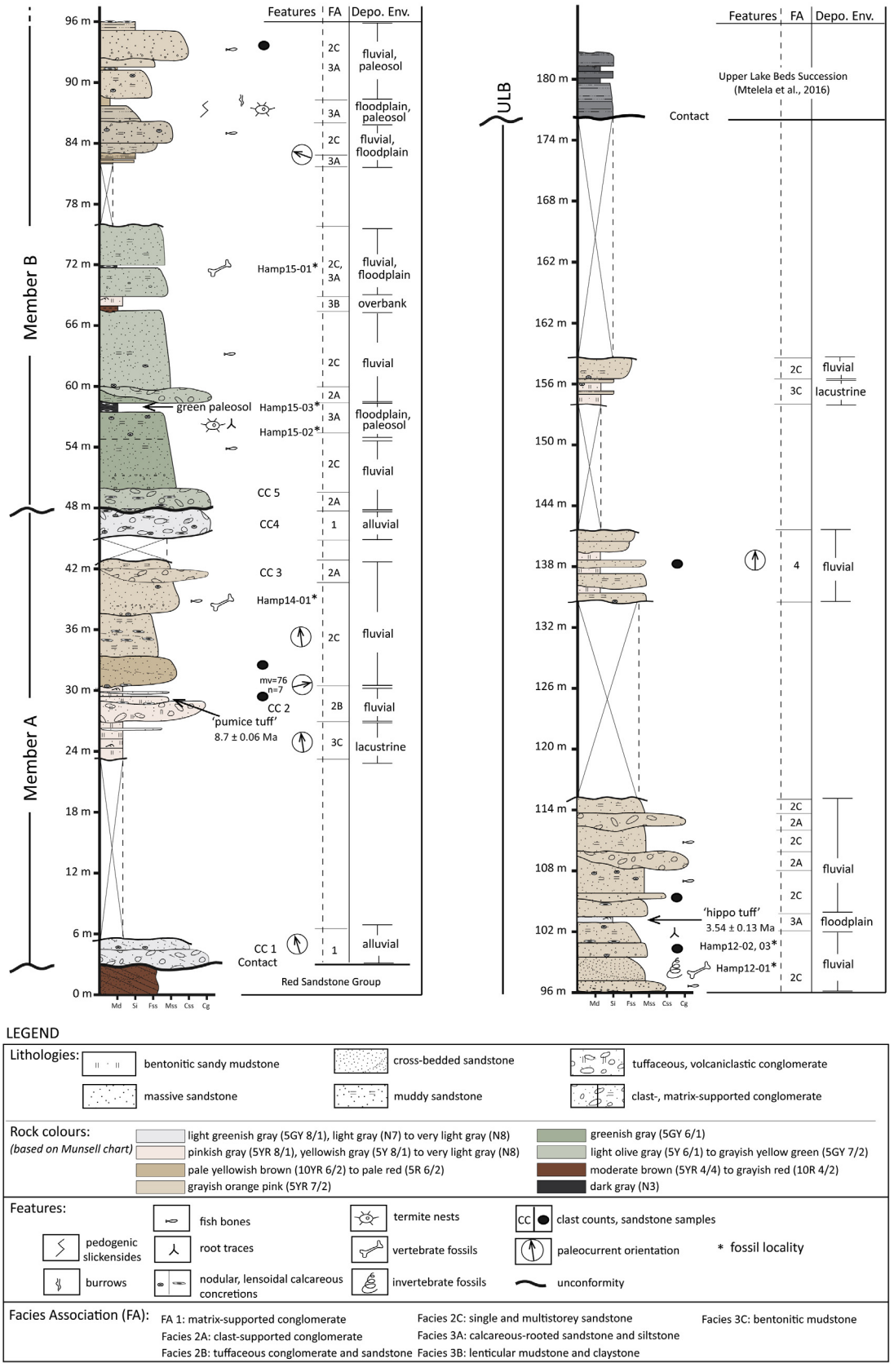


Fig. 3. Lower Lake Beds stratigraphic section measured along the Hamposia River drainage, from 8°37′54″S, 32°49′10″E to 8°34′35″S, 32°49′49″E. U-Pb age data for the Pumice Tuff and Hippo Tuff beds are from Hilbert-Wolf et al. (in press).

Table 1
Coarse-grained lithofacies in the Late Miocene-Pliocene lower Lake Beds.

Code	Lithofacies	Texture	Structures and features	Colour	Interpretation
Gcm	Clast-supported conglomerate	Clasts: pebble- to boulder-sized; comprised of vein quartz, metamorphic granitoids and meta-volcanic; poorly-sorted; sub-angular to rounded Matrix: fine- to medium-grained muddy sandstone	Massive to crudely-bedded; ungraded to weak normal grading	–	Unidirectional high-energy deposits
Gmm	Matrix-supported conglomerate	Clasts: pebble- to cobble-sized; monomictic: vein quartz dominated, or polymictic: comprising vein-quartz, metamorphic granitoids and meta-volcanics; typically poorly-sorted; Sub-angular to well rounded. Matrix: carbonaceous sandy mudstone or muddy sandstone	Typically massive; ungraded	Light greenish gray (5GY 8/1), very light gray (N8)	Unidirectional high-energy deposits
Gmv	Volcaniclastic conglomerate	Clasts: pebble- and less common cobble-sized; exclusively pumice in composition; poorly-sorted; sub-round to rounded Matrix: devitrified bentonitic ash	Massive; reversely graded	Pinkish gray (5YR 8/1), yellowish gray (5Y 8/1)	High-energy fluvial reworked pyroclastic or epiclastic deposits
Smp	Massive pebbly sandstone	Medium-grained muddy sand-to pebble-sized; moderate-poorly-sorted; quartzo-feldspathic in composition, with vein quartz dominated granules and pebbles; sub-angular to rounded; commonly characterized by discontinuous, 10-15 cm thick, lensoidal carbonate concretions	Massive to crudely-stratified; fish bones locally	Light greenish gray (5GY 8/1), pale red (5R 6/2)	Unidirectional medium- to high-energy deposits
Smv	Massive tuffaceous sandstone	Medium- to very coarse-grained sand and granules; moderate –well-sorted; sub-round to well-rounded; comprises pumice and vitric ash	Typically massive	Light gray (N7), very light gray (N8)	Unidirectional medium- to high-energy *epiclastic* deposits
Spv	Planar cross-stratified vitric-tuffaceous	Medium- to coarse-grained sand; moderately- to well-sorted; sub-round to well-sandstone rounded; comprises of pumice and vitric ash	Planar cross-stratified	Light gray (N7), very light gray (N8)	Unidirectional medium- to high-energy reworked pyroclastic deposits
Sm	Massive sandstone	Fine- to coarse-grained sand; quartz and feldspar dominated; moderately-poor-sorted; sub-angular to rounded	Massive or crudely-stratified; isolated carbonate nodules abundant fish bones locally	Pale yellowish brown (10YR 6/2), grayish yellow green (5GY 7/2), grayish orange pink (5YR 7/2), light olive gray (5Y 6/1), greenish gray (5GY 6/1)	Unidirectional low- to medium-energy deposits
Sh	Horizontally-stratified sandstone	Fine- to medium-grained sand; moderate-well-sorted; sub-angular to rounded; quartz and feldspar dominated	Horizontally-stratified	Light greenish gray (5GY 7/1), grayish orange pink (5YR 7/2)	Unidirectional low- to medium-energy deposits
St	Trough cross-stratified sandstone	Muddy, fine- to medium-grained sand; moderately-sorted; sub-angular to rounded	Trough cross-stratified; fish, crocodile and hippo remains	Grayish yellow green (5GY 7/2), pale yellowish brown (10YR 6/2)	Unidirectional low- to medium-energy deposits

Deposits of member B are characterized by alternating, multi-story clast-supported conglomerate and sandstone bodies that are locally interbedded or intercalated with thin (<60 cm thick) beds of fine-grained sandstone, siltstone, mudstone, and rare volcanic ash beds (10–20 cm thick). Conglomerate deposits are commonly massive tabular-lenticular bedded, typically cobble-sized and polymictic in composition. Sandstone lithofacies are generally quartzo-feldspathic (subarkosic), but vary in colour from greenish gray (5GY 6/1) or grayish yellow green (5GY 7/2) to grayish orange pink (5YR 7/2). A distinctive feature of this unit is the presence of well-developed paleosols with calcium carbonate accumulations (Bk horizons). Bedding is gently tilted across the middle portion of member B, dipping 5°–7° towards the north-northwest and west-northwest.

Member B is considerably more fossiliferous than member A and preserves abundant freshwater and terrestrial vertebrate remains in sandstone units. Isolated fish, crocodile and turtle remains are prolific in certain horizons throughout most of member B. In contrast, isolated large, exceptionally well-preserved mammalian and crocodilian cranial and post-cranial remains are locally abundant from both mudstone and sandstone bodies near the base and middle of member B.

5. Facies analysis

Fourteen sedimentary lithofacies were identified for the LLB in the Rukwa Rift Basin (Tables 1 and 2). Based on the repeated association of certain lithofacies together with distinctive internal and external geometries and diagnostic vertical and lateral facies relationships, seven facies assemblages were recognized and categorized into three genetically-related facies associations (FAs): alluvial fan deposits (FA1), fluvial channel deposits (FA2), and floodbasin deposits (FA3). In order of descending grain size, the specific facies assemblages include: matrix-supported conglomerates (FA1), clast-supported conglomerates (Facies 2A), tuffaceous conglomerate and sandstone (Facies 2B), single and multi-story

Table 2
Fine-grained lithofacies in Late Miocene-Pliocene lower Lake Beds.

Code	Lithofacies	Texture	Structures and features	Colour	Interpretation
Fhvs	Horizontally-stratified volcanic siltstone	Ash and silt-sized grains; with rare floating pumice sands	Horizontally stratified; crudely bedded in places	Medium dark-gray (N5) to light gray (N7)	Subaqueous pyroclastic flow/ fallout deposits
Fcvs	Current-rippled volcanic siltstone	Ash and silt-sized grains; with with isolated pumice sands and granules	Current and wave ripples	Medium dark-gray (N5) to light gray (N7)	Water-reworked pyroclastic flow deposits
Fr	Rooted fines	Muddy, silt- to fine-grained sand; moderately-sorted; locally contain isolated floating pebbles;	Massive: primary structures destroyed; calcified roots, calcareous nodules	Light greenish gray (5GY 8/1), pale red (5R 6/2)	Low-energy suspension deposits, paleosol
Fl	Finely-laminated mudstone, claystone	Clay- to silt-sized; rare isolated granules and pebbles; overall moderate-well-sorted	Fine-laminations; blocky weathering; rare isolated calcareous nodules	Moderate brown (5YR 4/4), grayish red (10R 4/2), very light gray (N8)	Low-energy suspension or traction deposits
Fcf	Massive fines	sandy mud, silt and clay; moderate-Well-sorted; locally organic	Typically massive; locally characterized by calcareous nodules	Grayish red (10R 4/2), very light gray (N8), dark gray (N3)	Low-energy suspension or overbank flood deposits
Fbr	Ripple-laminated bentonitic sandy mud-stone	Sandy ash-to silt-sized; composed of devitrified (bentonized) ash and pumice	Wavy, asymmetric ripples; local climbing ripples	Pinkish gray (5YR 8/1), light gray (N7), very light gray (N8)	Subaqueous low-energy water-lain pyroclastic flow deposits
Fbh	Horizontally-, crudely-stratified bentonitic sandy mudstone	Sandy-silty clay; moderate-well-sorted; devitrified (bentonitized) fine ash and pumices grains; lightly organic; rare calcareous nodules.	Horizontally to crudely stratified; mud cracks	Pinkish gray (5YR 8/1), light gray (N7), very light gray (N8)	Subaqueous low-energy pyroclastic/epiclastic suspension fallout deposits, with periodic sub-aerial exposure

sandstone (Facies 2C), calcareous, rooted sandstone and siltstone (Facies 3A), lenticular mudstone and claystone (Facies 3B) and bentonitic mudstone (Facies 3C). Each of these FAs is described in detail below, followed by interpretation of their depositional processes and environments (summarized in Table 3).

5.1. Facies association 1 – alluvial fan deposits

FA1 consists of 1.5–2.5 m thick tabular, matrix-supported conglomerate (Gmm) that mostly occurs as single beds or as beds that fine upward into massive sandstone facies (Sm) (Tables 1 and 3; Fig. 4A–B). FA1 is commonly defined by high-relief (>0.5 m) erosional-scours along bedding soles and/or tops. Conglomerate deposits (Gmm) are typically massive and characterized by poorly-sorted, sub-angular to sub-rounded pebbles and cobbles. Clast composition is dominated by vein-quartz and quartzite. Matrix support is the most characteristic feature of this FA, and is typically a sandy mud matrix; however, zones of clast-supported conglomerate (Gcm) are locally present. Both conglomerate (Gmm) and sandstone (Sm) facies of this FA are whitish in colour, ranging from light greenish gray (5GY 8/1), light gray (N7) to very light gray (N8). In places where FA1 occurs as a single thick conglomerate bed, crude upwarding fining is observed. Paleocurrent data deduced from pebble imbrication indicates northwest paleoflow. Calcium carbonate cement and nodular accumulations are very common in FA1, and are particularly dense towards the upper contacts. There are no fossils recovered from this FA.

5.2. Interpretation: FA1

FA 1 is interpreted to represent alluvial fan deposits based on texture and compositional features, including matrix composition, angularity of the clasts, poor sorting and crude upward fining. The overall coarse-grained nature, poor sorting and muddy matrix in the conglomerate are all indicative of high-energy bedload deposition by gravity-fallout processes associated with sheet floods or pseudoplastic debris flows (cf. Nemec, 1990; Leleu et al., 2009; Oyanyan et al., 2012). The common tabular geometry and moderately mature (texturally) nature of these debris flow deposits suggest alluvial sedimentation on the medial reaches (alluvial plain) of a channel system, where alluvial processes transition to proximal braided fluvial processes. The upward fining sandstone intervals of FA1 are interpreted to reflect waning flows of discrete flooding events.

Similar deposits in other areas have been interpreted to result from rapid uplift, weathering and erosion along faulted (rift) margins (Miall, 1981). The presence of dense calcium carbonate accumulations in these deposits likely indicates calcrete soil development, reflecting prolonged periods of aridity following the deposition (cf. Mack et al., 1993; Tanner, 2003). This interpretation is consistent with the observed high-relief erosion surfaces associated with this FA, which indicates hiatuses in sedimentation.

5.3. Facies association 2 – fluvial channel deposits

5.3.1. Facies 2A: clast-supported conglomerate

Facies 2A is relatively common in the study area, and dominated by 1–10 m thick tabular to lenticular clast-supported conglomerate (Gcm), interbedded or intercalated with minor matrix-supported conglomerate (Gmm) and sandstone facies (Smp, Sm, St) (Tables 1 and 3; Fig. 4A, C). Conglomerate beds pinch out laterally over a few meters to tens of meters. Bounding surfaces are typically erosional along bedding soles and gradational bedding tops. The conglomerate is typically massive or crudely stratified with weak normal grading and poorly-sorted pebble-to cobble-sized clasts and rare boulders. Conglomerates are polymictic, comprised of varied proportions of vein-quartz, meta-granitoids and meta-volcanic clasts. The matrix is typically fine-to medium-grained sandstone or, in places, very coarse-grained muddy sandstone. Facies 2A is repetitive across the study area, particularly in the

Table 3
Facies associations and depositional environments of Late Miocene-Pliocene lower Lake Beds.

Facies association	Facies	Diagnostic features	Architectural elements	Depositional process	Macrofossil	Depositional environment
FA 1 – Alluvial deposits						
	Gmm, (Sm)	Coarse-grained; massive; poorly sorted; crudely upward fining; matrix supported	SG, CH	Gravity settle-out from sheet floods or debris flows	–	Alluvial plain
FA 2 – Fluvial channel deposits						
Facies 2A	Gcm, Smp, (Sm)	Muddy, coarse-grained sand stone and conglomerate; poorly sorted; massive or crudely stratified; ungraded-to weakly normal-graded; erosive lower bounding surface	SG, CH	Debris flow, sheet flooding	–	Channel lags
Facies 2B	Gmv, Spv, Smv, Fhvs Fcvs, Fcf	High degree of sediment rounding; reverse grading; moderate-poorly sorted; interbedding of fine-grained devitrified ash and coarse-grained pumiceous sandstone	CH, FF(CH)	Debris flows, sheet floods, and suspension/ saturation settling of diluted hyperconcent rated flows	–	Fluvial/interfluvial channels
Facies 2C	Smp, Sm, Sh, St	High degree of sediment rounding; upward fining; erosive (lower bounding) surfaces	SG, CH, SB	Channel flow, sheet flooding, sediment-gravity fallout	Fish, hippo and crocodile remains	Fluvial channels
FA 3 – Floodbasin deposits						
Facies 3A	Sm, Fr	Massive–primary sedimentary structures destroyed; calcified roots; calcareous nodules	SB, FF	Fluvial channels, suspension and sediment-gravity fallouts	Trace fossils	Floodplain, paleosols
Facies 3B	Fl, Fcf, Fbh	Fine-grained sediments; finely laminated or massive; concave-up lower bounding surface	FF, FF (CH)	Suspension fallout	–	Abandoned channell fills
Facies 3C	Fbh, Fbr	Fine-grained sediments; plane or concave-up lower surface; finely laminated; locally slightly organic/ bioturbated;	FF, FF(CH), CH	Fluvial and interfluvial channel-fill, suspension fallout	–	small lakes/ponds

Architectural elements; SG = sediment-gravity flow, CH = channel fill, SB = sand bedform, FF = floodplain fines, including paleosol and overbank (after Miall, 1996).

middle portion of the measured stratigraphic sections along the Hamposia and Chizi River drainages, where facies 2A alternates with thick sandstone units of facies 2C. Paleocurrent analysis on cross-bedded sandstone and pebble imbrication in facies 2A indicates flow dominantly towards the north and northwest.

Facies 2A yields rare to abundant vertebrate fossil remains, particularly in the middle to upper portion of the stratigraphy, dominated by microsites and isolated cranial and post-cranial remains, although rare sites with associated bone concentrations also exist. The most abundant faunal remains are fish and aquatic vertebrates. Rare bivalves and gastropods are present. No wood or plant remains have been recovered from this facies, or from anywhere in the LLB.

5.3.2. Interpretation: facies 2A

Based on its coarse-grained nature, poor sorting, erosive basal surfaces, and absence of sedimentary structures, facies 2A is interpreted to represent basal lag and gravel bar deposits associated with large braided fluvial channels. This interpretation is consistent with the presence of common freshwater fossils. The intercalation of lenticular conglomerate and sandstone bedforms reflects hydrodynamic changes and lateral migration of channel-margins (e.g., Bridge et al., 2000; Umazamo et al., 2012), consistent with fluvial channel flow on the braidplain environments (Miall, 1996). The recurrence of facies 2A and alternation with sandstone deposits of facies 2C suggests multi-phase channel development.

5.3.3. Facies 2B: tuffaceous conglomerate and sandstone

Facies 2B deposits are typically 3–4 m thick and consist of dominantly matrix-supported tuffaceous conglomerate (Gmv) and volcaniclastic sandstones (Spv, Smv) (Tables 1–3; Fig. 5A–C). These facies are best developed along the Hamposia section, between 27 and 31 m above the basal contact with the Red Sandstone Group. The thickness of individual beds of facies 2B ranges from 25 cm to ~2 m. Upper and lower contacts are typically erosional. Tuffaceous conglomerate is typically massive, poorly sorted, and inversely graded. It is composed almost exclusively of pebble-to cobble-sized clasts of mostly reworked tuffaceous mudstone intraclasts and pumice clasts (devitrified now), which are sub-angular to round. Tuffaceous sandstone beds are massive (Smv) to planar cross-bedded (Spv), and composed of medium to coarse and very



Fig. 4. A) Outcrop photo of well-exposed alluvial-fluvial deposits along the Hamposia River section with illustrations of facies associations and major unconformity surfaces in the Lake Beds. **B-C)** Lower Lake Beds coarse-grained facies, including: massive, matrix-supported conglomerate (Gmm; **B**) and clast-supported conglomerate (Gcm; **C**). Note: arrow in Fig. 4A points to a high-relief erosional surface capping a thick calcareous paleosol, separating the lower and upper units (Member A and B) of the LLB succession.

coarse sand-sized pumice particles and fine ashy matrix, most of which has devitrified into clay, further lithifying these beds.

In many places, tuffaceous sandstone (Spv, Smv) is intercalated and/or interbedded with thin, tabular to lenticular beds of wave and ripple- or horizontally-stratified tuffaceous siltstone (Fcf, Fcvs, Fhvs; Fig. 5C–D). Deposits of this facies have distinctive pinkish gray (5YR 8/1), yellowish gray (5Y 8/1) or very light gray (N8) colours. Paleocurrent data measured on well-exposed tabular cross-stratification reveals northeast paleoflow. Contacts between conglomeratic lower portions of facies 2B and sandy-dominated upper intervals are typically erosional, and commonly marked by discontinuous, thin lenticular beds of calcium carbonate and

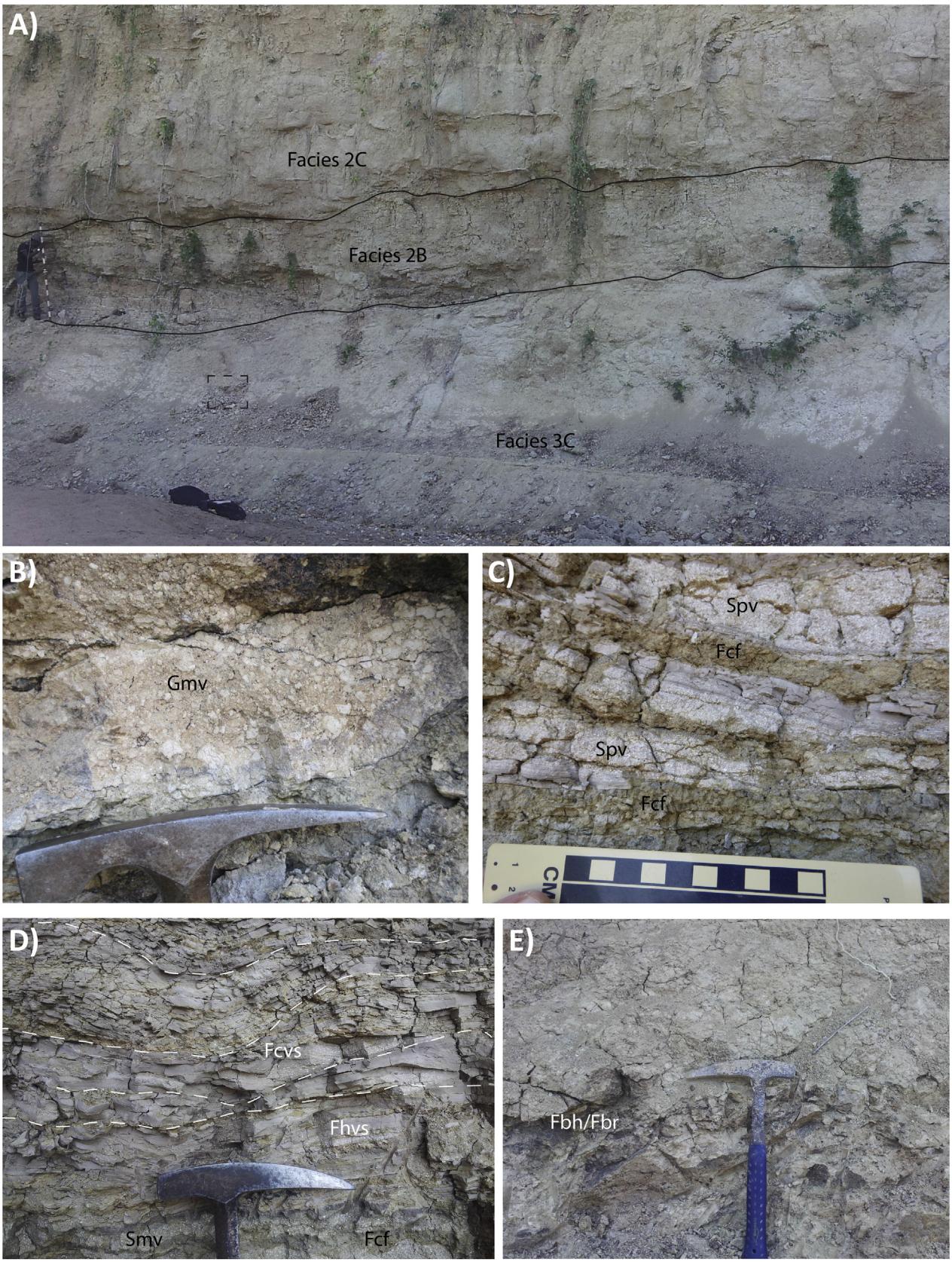


Fig. 5. A) Outcrop photo of fluvial-floodbasin/lacustrine volcanic and volcaniclastic flow deposits along the Hamposia river drainage, near Mpona Village. **B-E)** Close-ups images of: volcaniclastic conglomerate (Gmv; **B**); planar cross-stratified vitric-tuffaceous sandstone (Spv; **C**); current-ripple laminated and horizontally-stratified volcanic siltstone (Fcvs, Fhvs; **D**); and horizontal- and ripple-laminated bentonitic sandy mudstone (Fbh, Fbr; **E**).



Fig. 6. A) Photograph of a fossil-bearing, sand dominated fluvial channel deposits (FA2: Facies 2C) from the Hamposia section. **B-D**) Close-ups images of termite nest trace fossil (**B**), mammal fossils (**C**–**D**). Note an arrow in Fig. 6A pointing to a volcanic tuff bed (Hippo Tuff) dated at 3.54 ± 0.13 Ma (Hilbert-Wolf et al., in press).

calcareous nodular sandy concretions. Mud cracks are common in conglomerate, sandstone and mudstone beds. Similar to FA1, there are no fossils recovered from facies 2B.

5.3.4. *Interpretation: facies 2B*

Facies 2B is interpreted to represent fluvially reworked pyroclastic deposits. This interpretation is based on the high degree of sediment rounding and the interbedding of coarse-grained tuffaceous sandstone with devitrified ash (bentonite) and bentonitic mudstone deposits (e.g., Bhat et al., 2008). The ash-rich matrix and poorly-sorted nature of the conglomerate is indicative of debris flow-driven sedimentation. The deposition of this basal conglomerate resulted from sediment gravity settle-out during waning flow of a fluvial channel. A number of mechanisms have been put forth by various researchers to explain the reverse grading observed in some pyroclastic fallout and flow deposits (cf. Duffield et al., 1979 and references therein). The most plausible mechanism for the reverse-grading observed in these water-lain coarse pyroclastic deposits is related to clast density during gravity-debris-fallout, where large clasts were partially saturated and sank more slowly than smaller clasts (Sparks and Wilson, 1976). The presence of erosional upper surfaces of conglomeratic units and associated discontinuous carbonate lenses suggest channel abandonment and subaerial exposure. Deposition in the upper (sandstone-mudstone) interval of facies 2B most likely resulted from remobilized pyroclastic flow/fallout deposits from diluted hyperconcentrated fluvial flows (Bhat et al., 2008). The presence of wavy and ripple cross-laminated intervals (Fig. 5D) indicate current and wave-influenced deposition, suggesting sedimentation by subaqueous interfluvial channels or volcanic-clogged subaerial channels. This interpretation is also supported by different orientations observed for paleoflow in these deposits. Sandstone units within facies 2B resulted from relatively high-energy traction currents, whereas mudstone units were deposited by suspension settle-out during the waning stages of flows.

5.3.5. *Facies 2C: single and multi-story sandstone bodies*

Facies 2C is the most abundant FA in the upper interval of the LLB, and occurs repetitively within the stratigraphic sections along the Hamposia, Chizi and Ikumbi rivers. Facies 2C is defined by up to 7 m thick sequences composed of single or multiple sandstone bedsets of Sm, Smp, Sh and St, locally with gravel lenses (Gcm) (Tables 1 and 3; Fig. 6). Individual beds range from 50 cm to ~5 m thick. In most cases, facies 2C is characterized by a basal erosional contact and upward fining coarse-to medium-grained sandstone that is pebbly in places. Top surfaces are gradational to sharp, and are overlain by deposits of facies 3A. Facies 2C is locally eroded by, and overlain by, conglomeratic deposits of facies 2A. In places, individual beds and bedsets are bounded by 5–10 cm thick, discontinuous zones with carbonate concretions. Sandstones range in colour from brown, light brown to light green (see Munsell's rock colour codes in Fig. 3). Locally, facies 2C deposits are interbedded with lenticular, concave-up and laterally discontinuous mudstone beds and devitrified ash deposits of facies 3B.

Sandstone units of facies 2C are typically moderately to poorly sorted, and characterized by sub-angular to sub-rounded grains. Paleocurrent orientations, determined mainly from bedset dip-directions, indicate northerly (350-360°) paleoflow. Sandstone is typically quartzo-feldspathic in composition, locally containing isolated calcareous concretions. Facies 2C is fossiliferous,

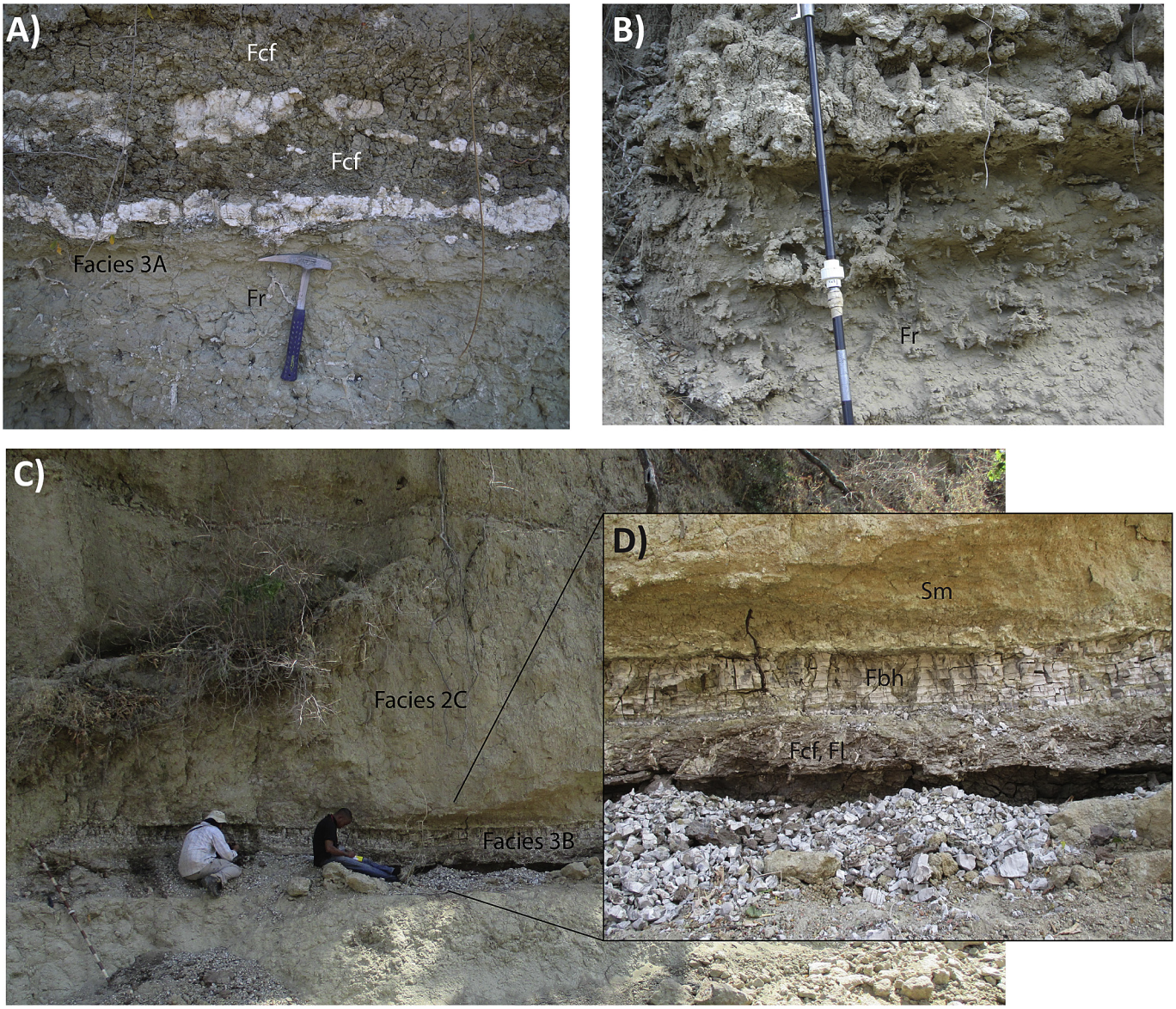


Fig. 7. Lower Lake Beds fine-grained facies. **A-B)** Calcareous, rooted sandstone, siltstone and mudstone (Facies 3A: Sm, Fr, Fcf facies). **C)** Lenticular, concave-up mudstone and claystone deposits (Facies 3B) interbedded with sandstone deposits of Facies 2C. **D)** Close-up images of Facies 3B; massive, finely-laminated mudstone and claystone (Fcf, Fl facies).

containing abundant fish bones, turtle, crocodilian, and large mammals (Fig. 6C and D) remains.

5.3.6. Interpretation: facies 2C

Single and multi-story sandstones of facies 2C are interpreted as fluvial channel deposits based upon their erosive basal contacts, textural features (sediment rounding and upward-fining), sedimentary structures and geometry. The typical upward fining trend from coarse-grained pebbly sandstone at the base to fine-grained sandstone at the top reflects typical channel-like vertical sediment accretion, associated with waning flow conditions within the channel. Facies 2C records a range of both normal flow and flood stage stream conditions. Flood stage conditions reflect rapid sediment deposition by gravitation collapse of bedload sediment from a flood-related debris channel flows as suggested by muddy and overall poor sediment sorting as well as thick and generally massive nature of many beds (Miall, 1996). However, in other portions of the stratigraphy, facies 2C more likely records more stable, continuous sedimentation from long lived perennial fluvial channels. The presence of abundant aquatic fauna (e.g., fish, turtles, crocodiles, and hippos) supports this interpretation. The spatial and temporal association of facies 2C with facies 3B and facies 2A deposits reflects subaerial exposure, channel abandonment and subsequent channel reactivation. Paleocurrent data and the association of these tabular and lenticular sandstone deposits with overbank channel-fill related deposits of facies 3B is interpreted to reflect deposition within a relatively large, low-sinuosity channel belt or braid-plain environment.

5.4. Facies association 3 – flood basin deposits

5.4.1. Facies 3A: calcareous, rooted sandstone and siltstone

Facies 3A is uncommon in the LLB and is characterized by 0.6–4 m thick, massive sandstone, siltstone and mudstone deposits (facies Sm, Fr, Fcf: Tables 1–3; Fig. 7A–B). The deposits occur as tabular to lenticular bedsets that are commonly defined by a sharp planar base and variably erosional to gradational top surfaces, upward fining and transitions into overlying mudstone beds. Facies 3A

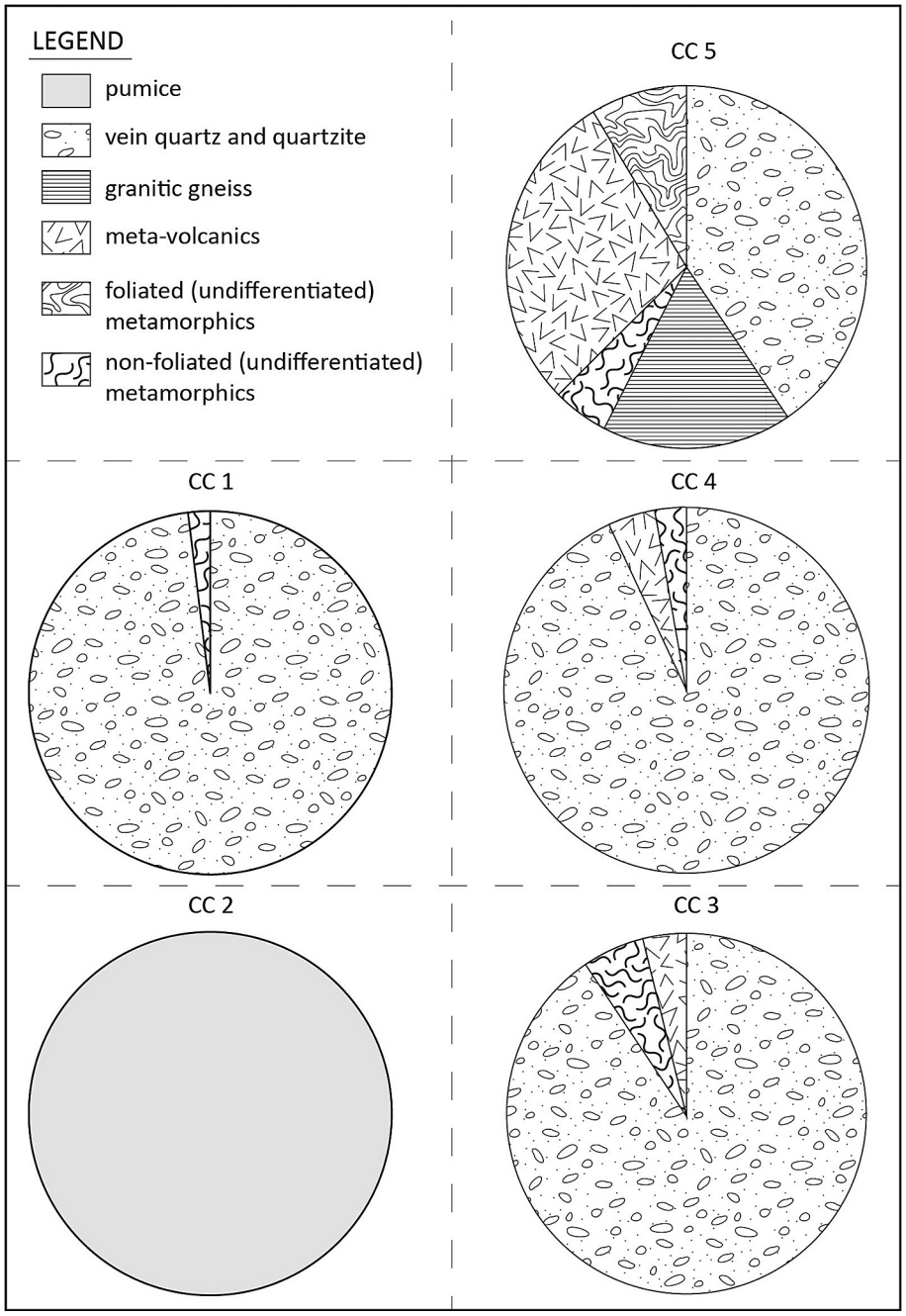


Fig. 8. Conglomerate pebble count results (CC1-CC5) for the LLB.

units extend laterally for meters to tens of meters, interfingering with facies 2C. Sandstone units (Sm) are medium-to fine-grained, moderately-sorted and quartzo-feldspathic in composition. Siltstone and mudstone units (facies Fr, Fcf) are commonly interbedded with thin, discontinuous lenses of calcium carbonates. Deposits of facies 3A tend to be heavily bioturbated with abundant calcified rootlets, burrows and nodular calcareous concretions. Rootlets vary in morphology between vertical and horizontal, and range in thickness from mm to few cm in diameter.

5.4.2. Interpretation: facies 3A

On the basis of lithofacies, geometry, and lateral relationship with major sandstone deposits (facies 2C), facies 3A deposits are interpreted to result from vertical sediment aggradation within a wide floodplain setting (e.g. Michaelsen et al., 2000). The massive nature of the deposits in this FA indicates that primary depositional structures were destroyed due to bioturbation. The presence of calcified rhizoliths and calcium carbonate concretions indicate that vegetation and associated soil development took place in a subaerial setting following deposition. Soil development is interpreted to have taken place in semi-arid climatic conditions, as evident by the presence of calcareous concretions and calcium carbonate lenses interbedded with mudstone facies in the upper parts of this facies.

5.4.3. Facies 3B: lenticular, concave-up mudstone and claystone

This FA is composed of 0.8–~1 m thick, lenticular units of claystone and mudstone (Fcf and Fl) that are locally interbedded

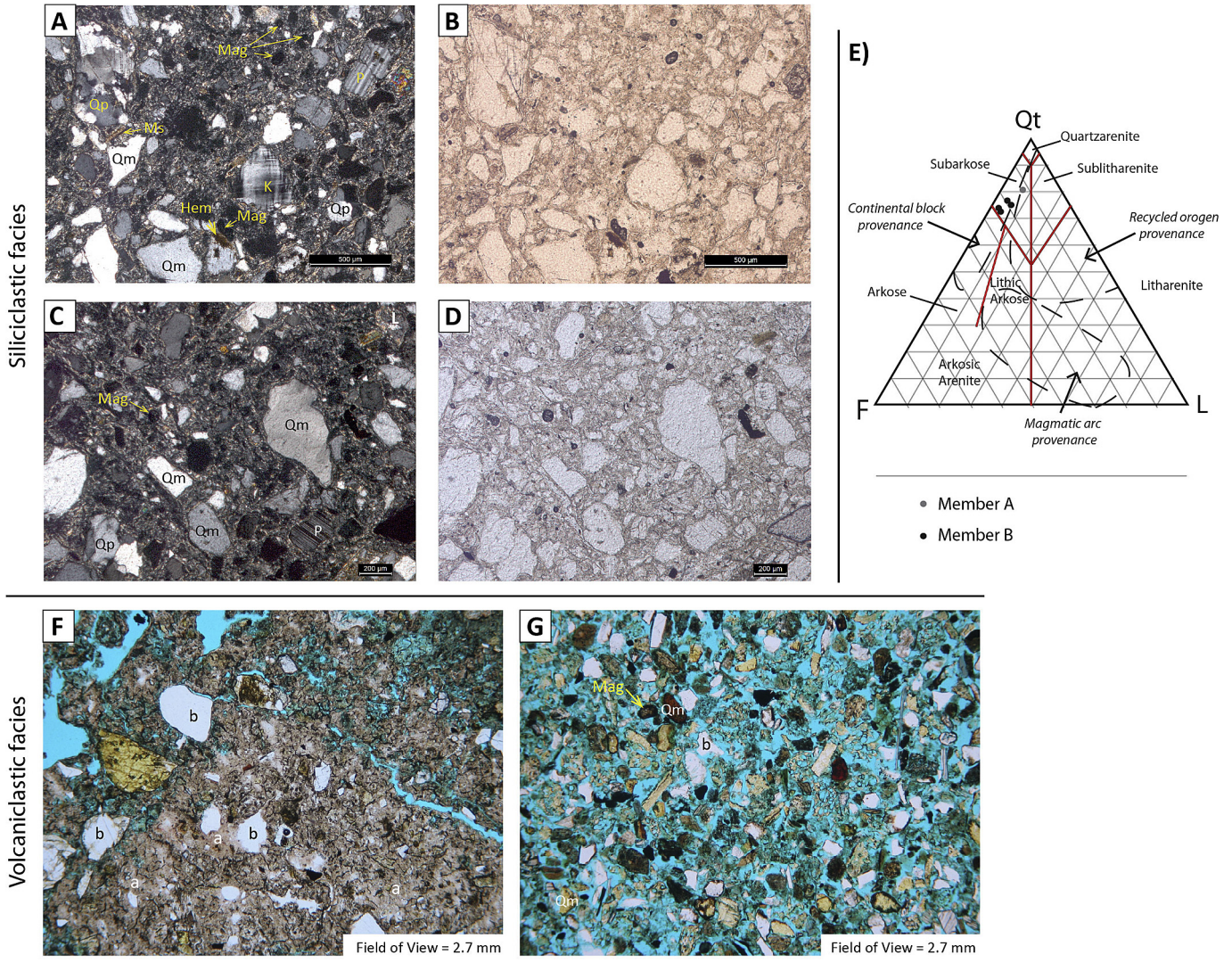


Fig. 9. Photomicrographs of the representative sandstone facies: microscopically-analyzed siliciclastic sandstone at crossed polarized **(A, C)** and plane polarized **(B, D)** light, with sandstone point count data plotted **(E)** (sandstone classification after Pettijohn, 1957); tuffaceous sandstone facies in plane polarized light **(F, G)**, comprising dominantly volcanic glass (a) and pumice grains (b).

with thin (<20 cm) siltstone beds (Fl) (Tables 1 and 3; Fig. 7C–D). These deposits are characterized by erosive, concave-up lower bounding surfaces and typically sharp upper contacts. Deposits of this facies occur in erosional scours that are most typically found above thick sandstone deposits of facies 2C. Individual beds in this FA range from 10 to 60 cm in thickness. Mudstone and claystone units are commonly moderate brown (5YR 4/4) or grayish red (10R 4/2). Claystone beds of this FA are typically brown in colour and massive, whereas the siltstone units are finely-laminated and locally contain isolated calcium carbonate concretions.

5.4.4. Interpretation: facies 3B

Facies 3B is interpreted to record low-energy, abandoned channel-fill deposition by suspension settling out of fine-grain sediments. This interpretation is mainly based on the fine-grained texture and concave-up geometry, as well as their spatial relationship with sandstone deposits of facies 2C. The presence of calcareous concretions in some intervals of this FA is interpreted to indicate periodic subaerial exposure and development of horizonated paleosols.

5.4.5. Facies 3C: bentonitic mudstone, bentonite and unweathered volcanic ash

This facies association is well-developed in the lower portion of the LLB and is less common stratigraphically up-section. Deposits of facies 3C form up to 4 m thick sheet-like packages of bentonitic mudstone, pure bentonites and unweathered ash beds (Fbh, Fbr, Fhvs; Tables 1 and 3; Fig. 5A, E), which are apparently laterally extensive. These mudstone units tend to be quite sandy and are dominantly composed of devitrified fine-grained ash and sub-rounded to well-rounded, silty-to very fine sand-sized pumice grains. They range in colour from pinkish gray (5YR 8/1), to yellowish gray (5Y 8/1) to very light gray (N8). Basal surfaces are poorly-exposed, but appear to exhibit concave-up geometry. The upper contact of this FA typically displays erosional scour from above (typically by FA 4). Individual beds of facies 3C range from 20 cm to 1.5 m, and include alternating parallel- and asymmetric ripple cross-laminated intervals. The lower interval of this FA appears to be massive and bioturbated. Intercalations of thin, lenticular, fine-grained sandstone (Sh) were observed near the upper limit of this FA.

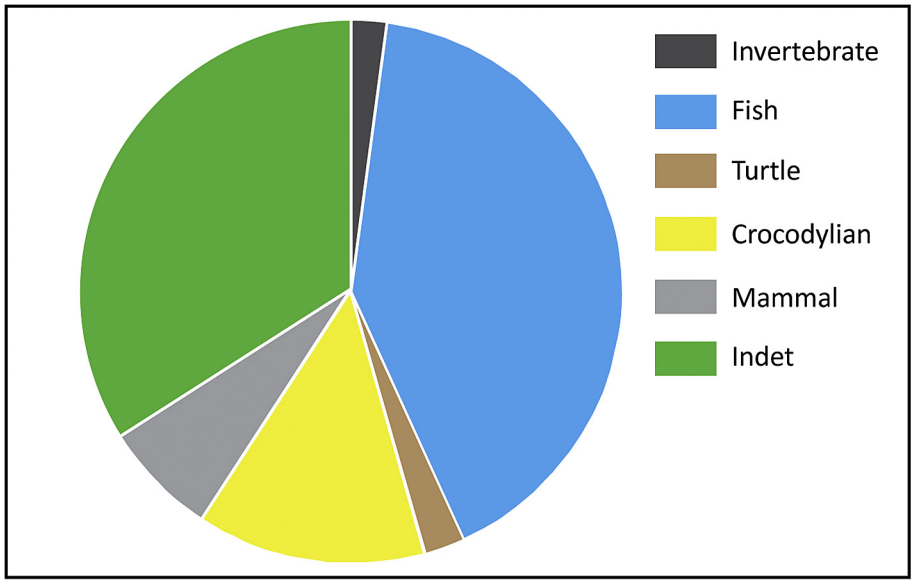


Fig. 10. Faunal composition based on fossils from Member B.

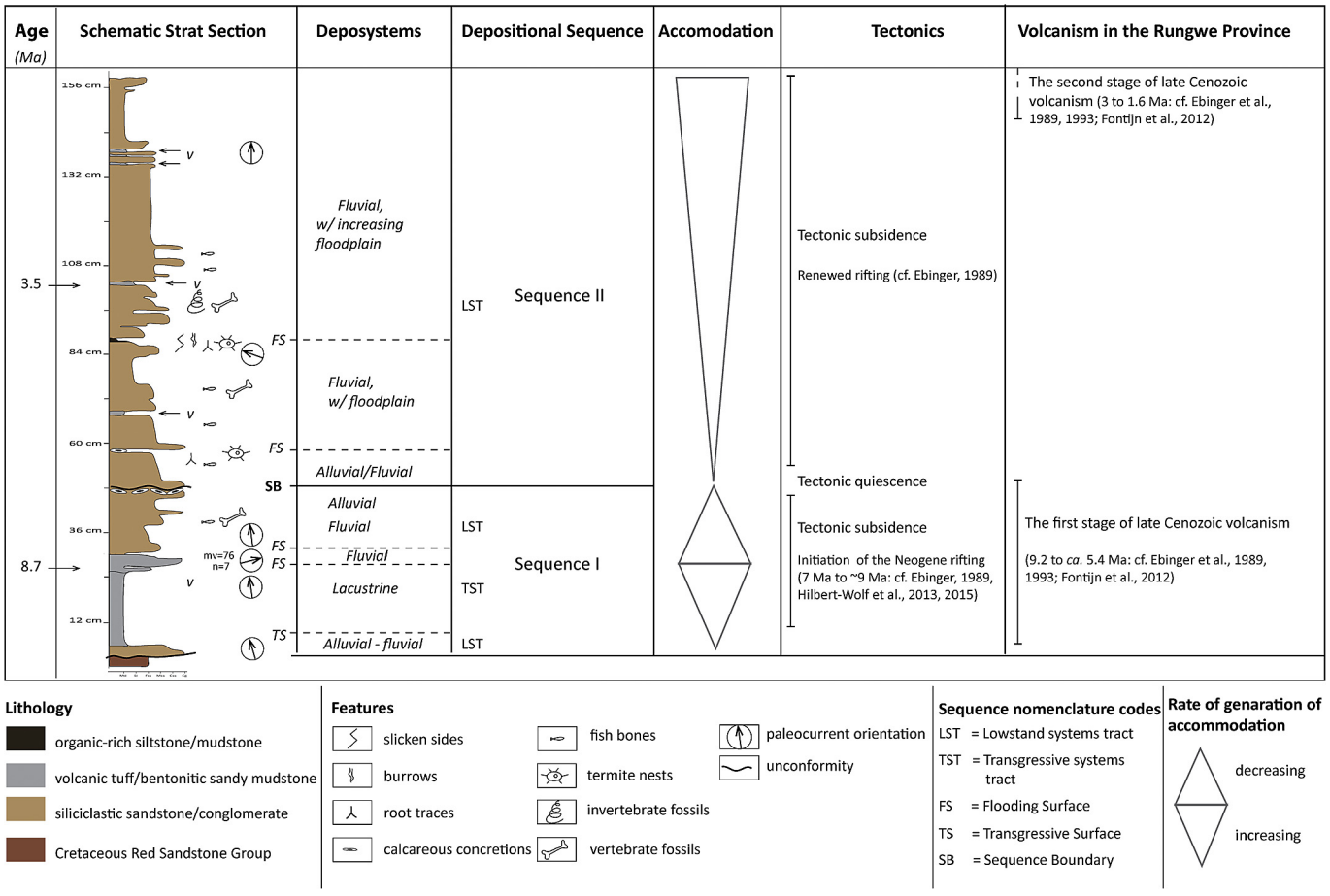


Fig. 11. Schematic stratigraphic section of the lower Lake Beds with sequence stratigraphic interpretations and inferred controls on sedimentation.

5.4.6. Interpretation: facies 3C

Based on the fine-grained size, thinly-laminated nature, geometry, and lateral extent, facies 3C is interpreted to record low-energy sedimentation within subaqueous flood basin ponds or small lakes (e.g., Talbot and Allen, 1996; Leleu et al., 2009; Umazamo et al., 2012). Textural features such as a high degree of rounding of individual silt-to fine-sand grains suggest sediment derivation from fluvial-reworked pyroclastic deposits in the

hinterlands (e.g., Cas and Wright, 1987; Nichols and Fisher, 2007; Bhat et al., 2008). Horizontally laminated beds (facies Fbh) were deposited by sediment settling from suspension. Ripple cross-laminated intervals of facies 3C suggests deposition from land-generated unidirectional and/or subaqueous current flows (e.g., Zavala et al., 2006, 2011; Cuitiño and Scasso, 2013). The deposits record a shallowing-upward trend, as demonstrated by overall coarsening upwards of this FA and intercalations of thin lenticular sandstone beds towards the upper limit of facies 3C, as well as spatial and temporal relationship with the overlying tuffaceous conglomerate deposits of facies 2B.

6. Sedimentary petrology

6.1. Conglomerate lithoclast composition

Pebble-counting was performed on five conglomerate beds (samples CC1 to CC5; Figs. 3 and 8), where all clasts >2cm in diameter were counted within a 50 cm^2 grid over each bed. The lithoclast compositions were grouped into five distinctive lithologic categories: pumice, vein quartz, granitic gneiss, meta-volcanics, foliated- and unfoliated metamorphic clasts.

The results show a major compositional shift mid-way through the stratigraphy that corresponds with the presence of a major erosional unconformity and calcrete horizon at ~45–48 m above the basal contact (Fig. 9). Below this horizon, siliciclastic conglomerate beds are dominated by vein-quartz clasts as demonstrated by clast-count samples CC1, CC3, and CC4. Statistically, lithoclast composition in the conglomerate beds of this lower interval shows that vein-quartz pebbles and cobbles make up 93–98% of the total counts, whereas the other 2–7% is composed of non-foliated metamorphic clasts. In contrast, above the unconformity, conglomerates beds are typically polymictic in composition. Although only one sample was counted formally (sample CC5: Fig. 8), visual inspection of conglomerate clast composition in the field and through analysis of field photographs indicate that other conglomerate units above the unconformity differ significantly in composition from those below this surface. The clast composition of sample CC5 is as follows: vein quartz and quartzite (~41%), meta-volcanic (~29%), granitic gneiss (17%), foliated metamorphic (6%) and non-foliated metamorphic (6%).

Besides the variation in siliciclastic conglomerate provenance between the lower and upper portions of the strata, the LLB succession is also characterized by volcaniclastic provenance variation across the stratigraphy. The lower stratigraphic interval contains volcaniclastic (tuffaceous) conglomerate deposits along with associated tuffaceous sandstone, vitric ash and bentonitic mudstones (Facies 2B). The tuffaceous conglomerate, which occur as a single bed and represented by sample CC2, is 100% pumice pebbles and cobbles that are cemented by a tuffaceous matrix, vitric ash and sandy to silt-sized pumice (Figs. 3, 5B and 8). Whereas the tuffaceous conglomerate bed is limited to this lower portion of the stratigraphy, the associated volcanic and volcaniclastic deposits decrease dramatically up-section, above the unconformity surface.

6.2. Sandstone petrology

Sandstone compositions in the LLB from the Hamposia River section vary between volcaniclastic and siliciclastic end members (Figs. 3 and 9). Volcaniclastic sandstones are less common, and occur as thin tabular or lenticular beds of pumice tuff (tuffaceous sandstone facies: facies 2B) that are limited to the lower part of the section. Siliciclastic sandstone compositions dominate the middle to upper part of the stratigraphic succession, and are associated with fluvial channel deposits (FA 2: facies 2C). Because of the very poorly indurated nature of the sandstones in the LLB, only a small suite of thin sections were made. Hence, the sandstone petrology must be considered preliminary and is largely based on hand sample description and analysis of five representative thin sections of the siliciclastic sandstone units, collected from across the stratigraphic section. A clear bias to this study has been the challenge of constructing quality thin sections of the volcaniclastic sandstone lithofacies, which are clay-rich and poorly cemented. However, volcaniclastic composition of these sandstone units is clear in limited thin sections and hand samples, and careful field observations confirm that this petrofacies is almost exclusively confined to the lower part of the LLB.

6.2.1. Siliciclastic petrofacies

On a Qt-F-L diagram (Fig. 9E), all thin-sectioned samples plot in the subarkose field. The results show that total quartz (including monocrystalline plus polycrystalline quartz) ranges from 75 to 81%; total feldspar (alkali and plagioclase) ranges between 12 and 23%; and total lithics range between 3 and 7%. The quartz grains exhibit both straight extinction and undulatory extinction. In all samples, monocrystalline quartz is dominant (66–89%) over polycrystalline quartz (11–33%). Plagioclase (constituting 7–17%; average 13%) dominates over potassium feldspars (3–9%; average 6%). Both plagioclase and potassium feldspar grains are mostly fresh, although there is a small component that does exhibit minor chemical alteration. These grains are primarily replaced by hematite along the edges. Lithics are dominated by metamorphic rock fragments (granitic gneiss and unfoliated meta-granitoids). Accessory minerals represent a few percent of the total grain fraction and include dense minerals (dominantly magnetite and garnet) and mica. Matrix varies from 4 to 10%, and porosity ranges between 6% and 10%. Cement varies between 8% and 18%, and is dominantly authigenic clays and hematite. Although the analyzed sandstone samples contain 8–18% cement, most sandstone units are less well cemented and moderately indurated.

6.2.2. Volcaniclastic petrofacies

As noted above, the volcaniclastic sandstone lithofacies produced few usable thin sections. However, it is clear that these samples range from nearly purely volcanic in nature to highly reworked with a large quartzose sand composition. Qualitative observations of thin-sectioned representative samples (Fig. 9F–G) reveals that volcaniclastic sandstone comprises dominantly pyroclastic material, most of which has weathered to clay minerals. However, relic pumice fragments are the most commonly observed framework grains and ranges from silt-to very coarse-grained sand sized. The second most abundant clast type are what appear to be lithic volcanic or volcaniclastic fragments composed of reworked volcanic siltstone and welded tuff fragments (Fig. 9F). Quartz and feldspar grains are locally abundant, and range from silt to fine grained-sand sized (Fig. 9G). Heavy minerals (mostly magnetite) and mica constitute minor proportions.

Volcaniclastic sandstone lithofacies are almost exclusively observed in the field in the lower part of the LLB, between the 23 and 31 m levels. A shift is observed in the siliciclastic conglomerate and sandstone petrology at the major erosional unconformity at 48 m. Below the boundary, in the volcaniclastic dominated succession, the siliciclastic sandstone lithofacies are typically quartzose at the base, and become more quartzo-feldspathic stratigraphically up-section, particularly above the boundary. Basal quartzose sandstone beds are whitish or very light gray (N8) in colour, whereas quartzo-feldspathic sandstone varies between brownish (pale yellowish brown, 10YR 6/2 to grayish orange pink, 5YR 7/2) and greenish (greenish gray, 5GY 6/1 to grayish yellow green, 5GY 7/2). This compositional change, which is readily

observable in the field, can also be depicted from the petrographically analyzed samples. Despite the fact that all samples plot on subarkose field on a Qt-F-L diagram, one sample collected from the lower interval (volcaniclastic interval), just below the unconformity surface, shows slightly higher abundance of quartz grains than the other samples collected above this horizon.

7. Faunal overview

Both members of the LLB strata preserve fossils, however, only fragmentary vertebrate specimens have been recovered from Member A. Member B appears more highly fossiliferous, with a total of 44 fossil specimens recovered as part of geological reconnaissance efforts in the (seven) most productive localities. Identifiable specimens (n = 29) are dominated by fishes (62%) and large crocodylians (21%), with smaller numbers of large bodied mammals (10%), turtles (3%) and mollusks (3%) (Fig. 10). Specimens range in size from <2 mm to over 60 cm in length. A detailed faunal description of the LLB materials is underway (N. Stevens, Pers. Comm.). Discoveries to date appear consistent with a marginal wetland located within a seasonally arid environment.

8. Sequence stratigraphic framework

We identify depositional sequences in the lower Lake Beds succession following a model-independent approach to sequence stratigraphy proposed by Catuneanu et al. (2011). In this study, a 156-m-thick stratigraphic section was measured along the western margin of the Rukwa Rift through the Hamposia River drainage (Figs. 2 and 3). This section preserves two distinctive depositional sequences in the lower Lake Beds succession in the RRB, which correspond closely with lithostratigraphic subidivisions (members A and B) defined for lower Lake Beds (Fig. 11). Stratal stacking patterns of the two sequences, termed Sequence I and Sequence II, reflect: 1) the transition of depositional environments from alluvial/fluvial-lacustrine to fluvial-floodplain dominated; 2) a shift in sedimentary provenance from volcaniclastic-to siliciclastic-dominated intervals; and 3) an apparent transition between sub-humid and semi-arid climatic conditions. Suggested climate changes are based on sandstone composition shifts from dominantly quartzose in Sequence I, to quartzo-feldspathic in Sequence II (cf. Roller et al., 2010), and a distinct increase in the presence and abundance of well-developed paleosols between the two sequences. A sequence bounding erosional unconformity (SB) is placed at the 48 m level in the Hamposia section, which clearly defines the contact between sequences I and II (Figs. 3 and 11). We integrate the facies architecture and sedimentology reported above, coupled with newly reported radioisotopic ages for the LLB (Hilbert-Wolf et al., in press), evidence for the timing and intensity of volcanism in the Rungwe Volcanic Province (Ebinger et al., 1989, 1993; Fontijn et al., 2012), and late Miocene to Pleistocene climate records for eastern Africa (deMenocal, 1995, 2004; Trauth et al., 2007; Roller et al., 2010) to understand and interpret controls on sedimentation in these two sequences.

8.1. Sequence I

Hilbert-Wolf et al. (in press) applied U-Pb geochronology to date two tuffs in the LLB, indicating that sequence I was deposited during the late Miocene, commencing by *ca* 8.7 ± 0.06 Ma. Sequence I represents the lower 48 m thick stratigraphic interval of the LLB, and corresponds to lithostratigraphic member A (Figs. 3 and 11). It is interpreted as an aggradational parasequence set of alluvial-fluvial (FAs 1 and 2) and lacustrine/floodbasin (Facies 3C) deposits that represent lowstand and highstand systems tracts, respectively. Sequence I is characterized by a basal low accommodation alluvial fan system that rapidly transitioned up section into a shallow, volcanically influenced lacustrine system with associated fluvial-deltaic deposition. This sequence most likely developed as a result of renewed rifting and increasing generation of accommodation space and increased sediment supply during the initiation of the Rungwe Volcanics. Facies stacking patterns support this concept. However, the basal ~3–23 m of this sequence is distinctly different from that of the rest of the sequence, dominated by a super-mature quartzose conglomerate reminiscent of the base of the Nsungwe Formation (basal few meters of the Utengule Member; Roberts et al., 2010). Roberts et al. (2012) interpreted the super-mature quartzose composition of the base of the Nsungwe Formation to reflect a major fluvial pediment surface associated with regional uplift during the initial development of the African Superswell. These workers documented a shift in detrital zircon provenance patterns, briefly reflecting a shift southward to northward provenance and paleoflow conditions. No such detrital zircon provenance patterns are recorded for this interval, but the similarity between the base of the Nsungwe and the base of the sequence I of the LLB is distinctive and is interpreted to represent a similar fluvial pediment surface associated with initiation of the LLB and reactivation of the rift system. This basal, super-mature quartzose interval of Sequence I is interpreted to represent a low-accommodation lowstand systems tract (LST) that developed as a result of initial reactivation of the Rukwa Rift around 8.7 Ma (Hilbert-Wolf et al., in press). These quartzose siliciclastic deposits are most likely sourced from quartz vein/pegmatitic, granitic and meta-granitoid terranes of the Archean Tanzanian Craton and Paleoproterozoic Ubendian belt (Quennell, 1956; Quennell et al., 1956; Daly et al., 1985), and probably partly recycling of the underlying Cretaceous RSG (Roberts et al., 2004, 2010). These deposits are capped by a calcareous paleosol horizon, which is more exposed in the basal LLB section along the Chizi River drainage (Fig. 2B). This distinctive paleosol horizon is interpreted to indicate subaerial exposure (cf. Scott and Smith, 2015) prior to rapid generation of accommodation and subsequent transition to a transgressive lacustrine/flood basin depositional system. This transition is also associated with a provenance shift from super mature quartzose conglomerate to immature volcaniclastic sandstones and siltstones. The sedimentary provenance shift and the deposition of primary and reworked pyroclastic deposits (FA2: facies 2B; and FA3: facies 3C) is associated with the first stage of late Cenozoic volcanism in the Rungwe Volcanic Province, between 9.2 and 5.4 Ma (Ebinger et al., 1989, 1993; Fontijn et al., 2012; Hilbert-Wolf et al., in press). A well-developed calcic paleosol caps the top of Sequence I.

The initial phase of super-mature alluvial sedimentation (LST) is envisaged to have developed as a result of uplift, weathering and erosion along the faulted basin margins during the opening phase of basin reactivation. This most likely resulted in pediment development prior to initiation of the Neogene EARS rifting cycle in the Western Branch (Ebinger, 1989; Ebinger et al., 1989). The transition from a fluvial pediment at the base of the sequence to a mosaic of small lakes and wetlands rimmed by proximal fluvial-deltaic channels (Facies 3C: ~23–27 m stratigraphic interval; Figs. 3 and 11) is interpreted to have resulted from an increase in the generation of accommodation space as rifting continued, contemporaneously with the initiation of the Rungwe Volcanic Province (Ebinger et al., 1989, 1993). A strong link to the initiation of the Rungwe volcanics is supported by the rapid influx of primary ash falls/flows and fluvially reworked (secondary) pyroclastic materials in this sequence. U-Pb dating of several of the volcanic tuffs in the LLB suggests a late Miocene age (8.7 ± 0.06 Ma) for the initiation of both volcanism and sedimentation in the RRB (Hilbert-Wolf et al., in press), which is consistent with the age of the oldest volcanics

dated in the Rungwe Volcanic Province by Ebinger (1989) and Ebinger et al. (1989). The uppermost portion of this sequence suggests decreasing volcanic input and transition to siliciclastic sand-dominated channel systems, suggesting a decrease of accommodation space in the basin. This is interpreted to indicate rapid filling of available accommodation space, followed by slow generation of accommodation and reduced sediment supply, perhaps associated with a period both volcanic and tectonic quiescence.

8.2. Sequence II

Sequence II is ~108 m thick and is characterized by fluvial channel-dominated deposits. Sequence II is interpreted to represent a regressive or lowstand system tract (LST) associated with a transition from a lacustrine to fluvial depositional system. Preliminary geochronologic and biostratigraphic data suggest that the deposition of Sequence II was initiated in the Pliocene (~4–3.5 Ma; Hilbert-Wolf et al., in press). Sedimentation may have continued into the Pleistocene; however no upper age brackets have been established for the top of this sequence. Channel deposits (FA2: facies 2A, 2C) in this sequence indicate a transition from high-energy, gravel-bed braided river systems to sandy braided river systems (Figs. 3 and 5). Floodplain deposits (FA3: facies 3A) are abundantly preserved and are characterized by well-developed paleosol horizons. Volcanic and volcaniclastic deposits are considerably less abundant in this sequence, and are limited to relatively thin beds of vitric tuff. The deposition of these volcaniclastic facies is associated with the second stage of late Cenozoic volcanism in the nearby Rungwe Volcanic Province that is constrained between 3 and 1.6 Ma (Ebinger et al., 1989, 1993; Fontijn et al., 2012). However, U-Pb ages obtained from these tuff beds (Hilbert-Wolf et al., in press) suggests that the second phase of volcanism in the Rungwe Province most likely extended back to ~4–3.5 Ma.

Sequence II is interpreted to have developed as a result of slow, but continuous generation of accommodation space that exceeded the rate of water and sediment infill. The generation of accommodation space in the basin is interpreted to have resulted from renewed rifting during the Pliocene-Pleistocene, which is associated with second episode of explosive volcanism in the RVP (Ebinger et al., 1989, 1993; Fontijn et al., 2012). This interpretation is also supported by cosmopolitan composition of siliciclastic sandstones and significant input of meta-volcanic and meta-granitoid clasts in conglomerate deposits of this sequence, suggesting unroofing (uplift, weathering and erosion) of metamorphic rocks along the rift flanks. The latter are most likely associated with the Paleoproterozoic Ubendian Belt (Daly et al., 1985). Base level fall and subsequent development of calcareous paleosol horizons, in addition to a relatively higher abundance of feldspars in siliciclastic sandstone of this sequence suggest generally arid climatic conditions during the deposition of this sequence, which is consistent with regional aridification trends reported elsewhere in eastern Africa during this time (e.g. deMenocal, 1995, 2004; Trauth et al., 2007; Roller et al., 2010).

9. Conclusions

We describe a newly discovered Miocene to Pliocene succession in the Rukwa Rift Basin of southwestern Tanzania, herein informally referred to as the lower Lake Beds. A detailed investigation of the stratigraphy and sedimentology of the deposits was conducted along the Hamposia River and other nearby drainages. Fourteen lithofacies were identified and categorized into seven genetically-related facies associations (FAs). A synthesis of vertical stacking patterns and lateral relationships of facies associations, along with sedimentary petrology and vertebrate fossil remains leads to a recognition of three main deposition environments: (1) alluvial environments, (2) fluvial channel environments, and (3) floodbasin environments, characterized by volcanic-filled lakes and ponds, abandoned channel-fills and floodplains. Petrologic investigations reveal a shifts between volcaniclastic and siliciclastic provenence in the lower portion of stratigraphy, to siliciclastic sandstones and polymictic conglomerates in the upper interval. This provides the basis for informally subdividing the succession into a volcaniclastic-dominated lower member A, and an overlying, siliciclastic dominated member B. Establishment of a formal stratigraphic subdivision and nomenclature for the Lake Beds Succession awaits further exploration across the basin to determine outcrop extent of the lower Lake Beds Succession, and a better outcrop-based and subsurface dating of these units.

Acknowledgements

We thank the Tanzania Petroleum Development Corporation (TPDC) and Heritage Oil Rukwa Tanzania Ltd. for providing a PhD bursary to the lead author (CM) and funding to conduct fieldwork in the Rukwa Rift Basin. This research was also supported by the US National Science Foundation (EAR_1349825, BCS_1127164), the National Geographic Society (CRE), and the post-graduate research fund from James Cook University. We are indebted to the staff of Heritage Oil Rukwa Tanzania Ltd in the Dar es Salaam office for support in the fieldwork logistics. We thank N. Boniface, J. Edmund, Z. Jinnah, and the Rukwa Rift Basin Project team members for their field assistance and valuable discussions. And lastly but not least, we are grateful to the Editor D. Delvaux and reviewers (including A. Cohen and R.Tucker) for constructive feedback that improved the manuscript.

References

Ashley, G.M., 2000. Geologists probe hominid environments. GSA Today Geol. Soc. Am. 10, 24–29.
Berger, L.R., 2012. Australopithecus sediba and the earliest origins of the genus Homo. J. Anthropol. Sci. 90, 1–16.
Berger, L.R., de Ruiter, D.J., Churchill, S.E., Schmid, P., Carlson, K.J., Dirks, P.H., Kibii, J.M., 2010. Australopithecus sediba: a new species of Homo-like australopith from South Africa. Science 328, 195–204.
Berger, L.R., Hawks, J., de Ruiter, D.J., Churchill, S.E., Schmid, P., Delezene, L.K., Kivell, T.L., Garvin, H.M., Williams, S.A., DeSilva, J.M., Skinner, M.M., Musiba, C.M., Cameron, N., Holliday, T.W., Harcourt-Smith, W., Ackermann, R.R., Bastir, M., Bogin, B., Bolter, D., Brophy, J., Cofran, Z.D., Congdon, K.A., Deane, A.S., Dembo, M., Drapeau, M., Elliott, M.C., Feuerriegel, E.M., Garcia-Martinez, D., Green, D.J., Gurtov, A., Irish, J.D., Kruger, A., Laird, M.F., Marchi, D., Meyer, M.R., Nalla, S., Negash, E.W., Orr, C.M., Radovcic, D., Schroeder, L., Scott, J.E., Throckmorton, Z., Tocheri, M.W., VanSickle, C., Walker, C.S., Wei, P., Zipfel, B., 2015. Homo naledi, a new species of the genus Homo from the Dinaledi Chamber, South Africa. eLife 4, e09560.
Betzler, C., Ring, U., 1995. Sedimentology of the Malawi rift: facies and stratigraphy of the Chiwondo beds, northern Malawi. J. Hum. Evol. 28, 23–35.
Bhat, G.M., Kundal, S.N., Pandita, S.K., Prasad, V.R., 2008. Depositional origin of tuffaceous units in the Pliocene upper Siwalik subgroup, Jammu (India), NW Himalaya. Geol. Mag. 145 (2), 279–294.
Bishop, W.W., 1978. Geological Background to Fossil Man: Recent Research in the Gregory Rift Valley, East Africa, vol. 6. Geological Society of London, Special Publications, pp. 1–4.
Bridge, J.S., Jalfin, G.A., Georgieff, S.M., 2000. Geometry, lithofacies, and spatial distribution of Cretaceous fluvial sandstone bodies, San Jorge basin, Argentina: outcrop analog for the hydrocarbon-bearing Chubut Group. J. Sediment. Res. 70, 341–359.
Bromage, T.G., Schrenk, F., Kaufulu, Z., 1985. Plio-Pleistocene deposits in Malawi's hominid corridor. Natl. Geogr. Soc. Res. Rep. 21, 51–52.
Bromage, T.G., Schrenk, F., Juwayeyi, Y.M., 1995a. Paleobiogeography of the Malawi rift: age and vertebrate paleontology of the Chiwondo beds, northern Malawi. J. Hum. Evol. 28, 37–57.
Bromage, T.G., Schrenk, F., Zonneveld, F.W., 1995b. Paleoanthropology of the Malawi Rift: an early hominid mandible from the Chiwondo Beds, northern Malawi. J. Hum. Evol. 28, 71–108.
Brown, F.H., 1981. Environments in the Lower Omo Basin from one to four million years ago. In: Rapp Jr., G., Vondra, C.F. (Eds.), Hominid Sites: Their Geologic

Settings. AAAS Symposium 63. Boulder: Westview, pp. 149–164.
Brown, F.H., Feibel, C.S., 1986. Revision of lithostratigraphic nomenclature in the Koobi Fora region, Kenya. J. Geol. Soc. Lond. 143, 297–310.
Brunet, M., Guy, F., Pilbeam, D., Lieberman, D.E., Likius, A., Mackaye, H.T., Ponce de Leon, M., Zollikofer, C.P.E., Vignaud, P., 2005. New material of the earliest hominid from the Upper Miocene of Chad. Nature 434, 752–755.
Brunet, M., Guy, F., Pilbeam, D., Mackaye, H.T., Likius, A., Ahounta, D., Beauvilain, A., Blondel, C., Bocherens, H., Boisserie, J.R., de Bonis, L., Coppens, Y., Dejax, J., Denys, C., Duringer, P., Eisenmann, V., Fanone, G., Fronty, P., Geraads, D., Lehmann, T., Lihoreau, F., Louchart, A., Mahamat, A., Merceron, G., Mouchelin, G., Otero, O., Pelaez-Campomanes, P., Ponce de Leon, M., Rage, J.C., Sapanet, M., Schuster, M., Sudre, J., Tassy, P., Valentin, X., Vignaud, P., Viriot, L., Zazzo, A., Zollikofer, C., 2002. A new hominid from the upper Miocene of Chad, Central Africa. Nature 418, 145–151.
Cas, R.A.F., Wright, J.V., 1987. Volcanic Successions: Modern and Ancient. Allen and Unwin, London.
Catuneanu, O., Galloway, W.E., Kendall, C.G.C., Miall, A.D., Posamentier, H.W., Strasser, A., Tucker, M.E., 2011. Sequence stratigraphy: methodology and nomenclature. Newletters Stratigr. 44/3, 173–245.
Chorowicz, J., Mukonki, M.B., 1980. Linéaments anciens, zones transformantes récentes et géotectonique des fossés dans l'est Africain, d'après la télédétection et la microtectonique. Royal Museum for Central Africa. Dep. Geol. Mineralogy Rapp. Ann Tervuren Belg. 1979, 143–146.
Clark, J.D., Hayness Jr., C.V., Mawby, F.E., Gautier, A., 1970. Interim report on paleoanthropological investigations in the Lake Malawi Rift. Quaternary 13, 305–354.
Cohen, A.S., Bocxlaer, B.V., Todd, J.A., McGlue, M., Michel, E., Nkotagu, H.H., Grove, A.T., Delvaux, D., 2013. Quaternary ostracodes and molluscs from the Rukwa Basin (Tanzania) and their evolutionary and paleobiogeographic implications. Palaeogeogr. Palaeoclimatol. Palaeoecol. 392, 79–97.
Crevecoeur, I., Skinner, M.M., Bailey, S.E., Gunz, P., Bortoluzzi, S., Brooks, A.S., Burlet, C., Cornelissen, E., Clerk, N.D., Maureille, B., Semal, P., Vanbrabant, Y., Wood, B., 2014. First early hominin from Central Africa (Ishango, Democratic Republic of Congo). PLoS One 9 (1), e84652.
Cuitiño, J.I., Scasso, R.A., 2013. Reworked pyroclastic beds in the early Miocene of Patagonia. Reaction in response to high sediment supply during explosive volcanic events. Sediment. Geol. 289, 194–209.
Daly, M.C., Klerkx, J., Nanyaro, J.T., 1985. Early Proterozoic terranes and strike-slip accretion in the Ubendian Belt of southwest Tanzania. Terra Cogn. 5, 257.
Delvaux, D., Kervyn, F., Macheyeki, A.S., Temu, E.B., 2012. Geodynamic significance of the TRM segment in the East African rift (W – Tanzania): active tectonics and paleostress in the Ufipa plateau and Rukwa basin. J. Struct. Geol. 37, 161–180.
Delvaux, D., Barth, A., 2010. African Stress Pattern from formal inversion of focal mechanism data. Implications for rifting dynamics. Tectonophysics 482, 105–128.
Delvaux, D., 2001. Tectonic and paleostress evolution of the Tanganyika-Rukwa-Malawi rift segment, East African rift system. In: Ziegler, P.A., Cavazza, W., Robertson, A.H.F., Crasquin-Soleau, S. (Eds.), Peri-Tethys Memoir 6: PeriTethyan Rift/Wrench Basins and Passive Margins. Mémoire Musée National Histoire Naturelle, vol. 186, pp. 545–567.
deMenocal, P., 1995. Plio-Pleistocene African climate. Sci. New Ser. 270, 53–59.
deMenocal, P., 2004. African climate change and faunal evolution during the Pliocene- Pleistocene. Earth Planet. Sci. Lett. 220, 3–24.
Dirks, P.H.G.M., Berger, L.R., Roberts, E.M., Kramers, J.D., Hawks, J., Randolph-Quinney, P.S., Elliott, M., Musiba, C.M., Churchill, S.E., de Ruiter, D.J., Schmid, P., Backwell, L.R., Belyanin, G.A., Boshoff, P., Hunter, K.L., Feuerriegel, E.M., Gurtov, A., du, G., Harrison, J., Hunter, R., Kruger, A., Morris, H., Makhubela, T.V., Peixotto, B., Tucker, S., 2015. Geological and taphonomic evidence for deliberate body disposal by the primitive hominin species Homo naledi from the Dinaledi Chamber, South Africa. eLife 4, e09651.
Dirks, P.H., Kibii, J.M., Kuhn, B.F., Steininger, C., Churchill, S.E., Kramers, J.D., Pickering, R., Farber, D.L., Meriaux, A.S., Herries, A.I., King, G.C., Berger, L.R., 2010. Geological setting and age of Australopithecus sediba from Southern Africa. Science 328, 205–208.
Duffield, W.A., Bacon, C.R., Roquemore, G.R., 1979. Origin of reserve-graded bedding in air-fall pumice, Coso Range, California. J. Volcanol. Geotherm. Res. 5, 35–48.
Dunkleman, T., 1986. The Structural and Stratigraphic Evolution of Lake Turkana. Thesis. Duke University, Durham, N.C., 64 p.
Ebinger, C.J., Deino, A.L., Tesha, A.L., Becker, T., Ring, U., 1993. Tectonic controls on rift basin morphology – evolution of the northern Malawi (Nyasa) Rift. J. Geophys. Res. 98, 17821–17836.
Ebinger, C.J., 1989. Tectonic development of the western branch of East African rift system. Geol. Soc. Am. Bull. 101, 885–903.
Ebinger, C., Deino, A., Drake, R., Tesha, A., 1989. Chronology of volcanism and rift basin propagation: Rungwe volcanic Province, East Africa. J. Geophys. Res. 94, 15785–15803.
Feibel, C.S., 2011. A geological history of the Turkana basin. Evol. Anthropol. 20 (6), 206–216.
Feibel, C.S., Harris, J.M., Brown, F.H., 1991. Palaeoenvironmental context for the late. Neogene of the Turkana basin. In: Harris, J.M. (Ed.), Koobi Fora Research Project, vol. 3. Clarendon, Oxford, pp. 321–370.
Fleagle, J.G., Rasmussen, D.T., Yirga, S., Bown, T.M., Grine, F.E., 1991. New hominid fossils from Fejej, Southern Ethiopia. J. Hum. Evol. 21, 145–152.
Fontijn, K., Williamson, D., Mbede, E., Ernst, G.G.J., 2012. The Rungwe Volcanic Province, Tanzania—a volcanological review. J. Afr. Earth Sci. 63, 12–31.
Grantham, D.R., Teale, E.O., Spurr, A.M., Harkin, D.A., Brown, P.E., 1958. Quarter Degree Sheet 244 (Mbeya). Geological Survey of Tanganyika, Dodoma.
Haberyan, K.A., 1987. Fossil diatoms and the paleolimnology of Lake Rukwa, Tanzania. Freshw. Biol. 17, 429–436.
Haile-Selassie, Y., Gibert, L., Melillo, S.M., Ryan, T.M., Alene, M., Deino, A., Levin, N.E., Scott, G., Saylor, B.Z., 2015. New species from Ethiopia further expands Middle Pliocene hominin diversity. Nature 521, 483–488.
Hautot, S., Tarits, P., Whaler, K., Le Gall, B., Tiercelin, J.J., Le Turdu, C., 2000. Deep structure of the Baringo Rift Basin (Central Kenya) from three-dimensional magnetotelluric imaging: implications for rift evolution. J. Geophys. Res. 105, 23,493–23,518.
Herries, A.I.R., Adams, J.W., 2013. Clarifying the context, dating and age of the Gondolin hominins and paranthropus in South Africa. J. Hum. Evol. 65, 676–681.
Hilbert-Wolf, H.L., Roberts, E.M., Mtelela, C., O'connor, P.M., Stevens, N.J., 2013. Constraining the timing of Cenozoic rifting and basin development in the Rukwa Rift Basin of the East African Rift System via detrital zircon geochronology. In: 125th Anniversary of GSA, Annual Meeting in Denver, U.S.A.
Hilbert-Wolf, H., Roberts, E.M., Downie, R., Mtelela, C., Stevens, N., O'Connor, P., 2016. Application of U-Pb detrital zircon geochronology to drill cuttings for age control in hydrocarbon exploration wells: a case study from the Rukwa Rift Basin, Tanzania. AAPG Bull. (in press).
Ingersoll, R.V., Bullard, T.F., Ford, R.L., Grimm, J.P., Pickle, J.D., Sares, S.W., 1984. The effect of grain size on detrital modes: a test of the Gazzi-Dickinson point-counting method. J. Sediment. Petrol. 54, 103–116.
Kazmin, V., 1980. Transform faults in the East African rift system. In: Geodynamic Evolution of the Afro-Arabian Rift System, vol. 47. Atti dei convegni Lincei, Accademia Nazionale dei Lincey, Roma, pp. 65–73.
Kilembe, E.A., Rosendahl, B.R., 1992. Structure and stratigraphy of the Rukwa rift. Tectonophysics 209, 143–158.
Kingston, J.D., 2007. Shifting adaptive landscapes: progress and challenges in reconstructing early hominid environments. Am. J. Phys. Anthropol. Suppl. Yearb. Phys. Anthropol. 134 (Suppl. 45), 20–58.
Kullmer, O., Sandrock, O., Kupczik, K., Frost, S.R., Volpato, V., Bromage, T.G., Schrenk, F., 2011. New primate remains from Mwenirondo, Chiwondo beds in northern Malawi. J. Hum. Evol. 61, 617–623.
Lawley, C.J.M., Selby, D., Condon, D.J., Horstwood, M., Millar, I., Crowley, Q., Imber, J., 2013. Lithogeochemistry, geochronology and geodynamic setting of the Lupa Terrane, Tanzania: implications for the extent of the Archean Tanzanian Craton. Precambrian Res. 231, 174–193.
Leakey, M.G., Feibel, C.S., McDougall, I., Walker, A., 1995. New four-million-year- old hominid species from Kanapoi and AlliaBay, Kenya. Nature 376, 565–571.
Leakey, L.S.B., Leakey, M.D., 1964. Recent discoveries of fossil hominids in Tanganyika: at Olduvai and near lake Natron. Nature 202, 5–7.
Leleu, S., Hartley, A.J., Williams, B.P.J., 2009. Large-scale alluvial architecture and correlation in a Triassic pebbly braided river system, lower Wolfville formation (fundy basin, Nova Scotia, Canada). J. Sediment. Res. 79, 265–286.
Lockwood, C.A., Tobias, P.V., 1999. A large hominin cranium from Sterkfontein, South Africa and the status of Australopithecus africanus. J. Hum. Evol. 36, 637–685.
Mack, G.H., James, W.C., Monger, H.C., 1993. Classification of paleosols. Geol. Soc. Am. Bull. 105, 129–136.
Maslin, M.A., Brierley, C.M., Milner, A.M., Shultz, S., Trauth, M.H., Wilson, K.E., 2014. East African climate pulses and early human evolution. Quat. Sci. Rev. 101, 1–17.
Maslin, M.A., Christensen, B., 2007. Tectonics, orbital forcing, global climate change, and human evolution in Africa. J. Hum. Evol. 53, 443–464.
Mbede, E.I., 1993. Tectonic development of the Rukwa Rift Basin in SW Tanzania. Berl. Geowiss. Abh. 152, 92 p.
Menter, C.R., Kuykendall, K.L., Keyser, A.W., Conroy, G.C., 1999. First record of hominid teeth from the Plio-Pleistocene site of Gondolin, South Africa. J. Hum. Evol. 37, 299–307.
Miall, A.D., 1996. The Geology of Fluvial Deposits: Sedimentary Facies, Basin Analysis, and Petroleum Geology. Springer-Verlag, Berlin, New York, 582 p.
Michaelsen, P., Henderson, R.A., Crosdale, P.J., Mikkelsen, S.O., 2000. Facies architecture and depositional dynamics of the Upper Permian rangal coal measures, Bowen basin, Australia. J. Sediment. Res. 70, 879–895.
Morley, C.K., 2010. Stress re-orientation along zones of weak fabrics in rifts: an explanation for pure extension in 'oblique' rift segments? Earth Planet. Sci. Lett. 297, 667–673.
Morley, C.K., Cunningham, S.M., Harper, R.M., Westcott, W.A., 1999. Geology and geophysics of the Rukwa rift, East Africa. In: Morley, C.K. (Ed.), Geoscience of Rift Systems- Evolution of East Africa. American Association of Petroleum Geologists, Studies in Geology, 44, pp. 91–110.
Morley, C.K., Cunningham, S.M., Harper, R.M., Wescott, W.A., 1992. Geology and geophysics of the Rukwa rift, East Africa. Tectonics 11, 68–81.
Mtelela, C., Roberts, E.M., Downie, R., Hendrix, M.S., 2016. Interplay between structural, climatic, and volcanic controls on quaternary lacustrine-deltaic sedimentation patterns in the Western branch of the East African rift system, Rukwa rift, Tanzania. J. Sediment. Res. 86, 1179–1207.
Nemec, W., 1990. In: Colella, A., Prior, D.B. (Eds.), Aspects of Sediment Movement on Steep Delta Slopes. in: Coarse-grained Deltas, vol. 10. International Association of Sedimentologists, Special Publication, pp. 29–73.
Nichols, G.J., Fisher, J.A., 2007. Processes, facies and architecture of fluvial distributary systems deposits. Sediment. Geol. 195, 75–90.
O'Connor, P.M., Gottfried, M.D., Stevens, N.J., Roberts, E.M., Ngasala, S., Kapilima, S.,

Chami, R., 2006. Dinosaurs and other vertebrates from the Cretaceous red sandstone group, Rukwa Rift Basin, Southwestern Tanzania. J. Afr. Earth Sci. 44, 277–288.
O'Connor, P.M., Sertich, J.J.W., Stevens, N.J., Roberts, E.M., Gottfried, M.D., Hieronymus, T.L., Jinnah, Z.A., Ridgely, R., Ngasala, S.E., Temba, J., 2010. The evolution of mammal-like crocodyliforms in the Cretaceous Period of Gondwana. Nature 466, 748–751.
Oyanyan, R.O., Soronnadi-Ononiwu, C.G., Omoboriowo, A.O., 2012. Depositional environments of sam-bis oil field reservoir sands, Niger Delta, Nigeria. Pelagia Research Library. Adv. Appl. Sci. Res. 3, 1624–1638.
Pettijohn, F.J., 1957. Sedimentary Rocks, second ed. Harper & Brothers, New York, p. 718.
Pickering, R., Hancox, P.J., Lee-Thorp, J.A., Grun, R., Mortimer, G.E., McCulloch, M., Berger, L.R., 2007. Stratigraphy, U-series chronology and palaeoenvironments at Gladysvale Cave: insights into the climatic control over South African hominin bearing cave deposits. J. Hum. Evol. 53, 602–619.
Pickford, M., Senut, B., Hadoto, D., 1993. Geology and Palaeobiology of the Albertine Rift Valley, Uganda-Zaire, vol. I. Geology. Orléans: C.I.F.E.G. 190 p.
Potts, R., 1998. Environmental hypothesis of hominin evolution. Yearb. Phys.Anthropol. 41, 93–136.
Quennell, A.M., 1956. 1:2,000,000 Geological Map of Tanzania.
Quennell, A.M., Mcinley, A.C.M., Aitken, W.G., 1956. Summary of the geology of Tanganyika. Geol. Surv. Tanganyika Mem. 1, 264 p.
Roberts, E.M., O'Connor, P.M., Gottfried, M.D., Stevens, N.J., Kapalima, S., Ngasala, S., 2004. Revised stratigraphy and age of the red sandstone group in the Rukwa Rift Basin, Tanzania. Cretac. Res. 25, 749–759.
Roberts, E.M., O'Connor, P.M., Stevens, N.J., Gottfried, M.D., Jinnah, Z.A., Ngasala, S., Choh, A.M., Amstrong, R.A., 2010. Sedimentology and depositional environments of the red sandstone group, Rukwa Rift Basin, southwest Tanzania: new insights into Cretaceous and Paleogene terrestrial ecosystems and tectonics in sub-equatorial Africa. J. Afr. Earth Sci. 57 (3), 179–212.
Roberts, E.M., Stevens, N.J., O'Connor, P.M., Dirks, P.H.G.M., Gottfried, M.D., Clyde, W.C., Armstrong, R.A., Kemp, A.I.S., Hemming, S., 2012. Initiation of the western branch of the East African Rift coeval with the eastern branch. Nat. Geosci. 5, 289–294.
Roller, S., Hornung, J., Hinderer, M., Ssemmanda, I., 2010. Middle Miocene to Pleistocene sedimentary record of rift evolution in the southern Albert Rift (Uganda). Int. J. Earth Sci. 99, 1643–1661.
Rozzi, F.V.R., Bromage, T., Schrenk, F., 1997. UR 501, the Plio-Pleistocene hominid from Malawi. Analysis of the microanatomy of the enamel. Earth Planet. Sci. 325, 231–234.
Sandrock, O., Kullmer, O., Schrenk, F., Yuwayeyi, Y.M., Bromage, T.G., 2007. Fauna, taphonomy and ecology of the Plio-Pleistocene Chiwondo beds, Northern Malawi. In: Bobe, R., Alemseged, Z., Behrensmeyer, A.K. (Eds.), Hominin Environments in the East African Pliocene: an Assessment of the Faunal Evidence. Springer, Dordrecht, pp. 315–332.
Scott, J.J., Smith, M.E., 2015. Trace fossils of the eocene green river Lake basins, Wyoming, Utah, and Colorado. In: Smith, M.E., Carroll, A.R. (Eds.), Stratigraphy and Paleolimnology of the Green River Formation, Western USA. Syntheses in Limnology 1. http://dx.doi.org/10.1007/978-94-017-9906-5_12.
Sepulchre, P., Ramstein, G., Fluteau, F., Schuster, M., 2006. Tectonic uplift and Eastern Africa aridification. Science 313, 1419–1423.
Sherwood, R.J., Kingston, J.D., 2002. Paleoanthropological survey of the Lake Rukwa basin, Tanzania. Am. J. Phys. Anthropol. Suppl. 34, 141 p.
Spandler, C., Hammerli Sha, P., Hilbert-Wolf, H.L., Roberts, E.M., Schmitz, M., 2016. MKED1: a new titanite standard for in situ microanalysis of trace elements, Sm-Nd isotopes, and U-Pb geochronology. Chem. Geol. 425, 110–126.
Sparks, R.S.J., Wilson, L., 1976. A model for the formation of ignimbrite by gravitational column collapse. J. Geol. Soc. Lond. 132, 441–451.
Stanley, S.M., 1995. Climatic forcing and the origin of the human genus. In: Effects of Past Global Change in Life. National Research Council, Washington, DC, pp. 233–243. National Academy Press, Studies in Geophysics.
Stevens, N.J., Gottfried, M.D., Roberts, E.M., Ngasala, S., Kapilima, S., O'Connor, P.M., 2008. Paleontological exploration of Africa: a view from the Rukwa Rift Basin of Tanzania. In: Fleagle, J.G., Gilbert, C.C. (Eds.), Elwyn Simmons: A Search for Origins. Developments in Primatology. Progress and Prospects. Springer, pp. 159–180.
Stevens, N.J., Seiffert, E.R., O'connor, P.M., Roberts, E.M., Schmitz, M.D., Krause, C., Gorscak, E., Gasala, S., Hieronymus, T.L., Joseph, T., 2013. Palaeontological evidence for an Oligocene divergence between Old World monkeys and apes. Nature 497, 611–614.
Stewart, K.M., Murray, A.M., 2013. Earliest fish remains from the Lake Malawi Basin, Malawi, and biogeographical implications. J. Vertebrate Paleontol. 33, 532–539.
Stollhofen, H., Stanistreet, I.G., McHenry, L.J., Mollel, G.F., Blumenschine, R.J., Masao, F.T., 2008. Fingerprinting facies of the Tuff IF marker, with implications for early hominin palaeoecology, Olduvai Gorge, Tanzania. Palaeogeogr. Palaeoclimatol. Palaeoecol. 259, 382–409.
Susman, R.L., de Ruiter, D.J., 2004. New hominin first metatarsal (SK 1813) from Swartkrans. J. Hum. Evol. 47, 171–181.
Talbot, M.R., Allen, P.A., 1996. Lakes. In: Reading, H.G. (Ed.), Sedimentary Environments: Processes, Facies and Stratigraphy. Blackwell Science, Cambridge, pp. 83–124.
Tanner, L.H., 2003. Pedogenic features of the Chinle group, four corners region: evidence Late Triassic aridification. In: New Mexico Geological Society Guidebook, 54th Field Conference, Geology of the Zuni Plateau,, pp. 269–280.
Theunissen, K., Klerkx, J., Melnikov, A., Mruma, A., 1996. Mechanism of inheritance of rift faulting in the western branch of the East African Rift, Tanzania. Tectonics 15 (4), 776–790.
Tiercelin, J.J., Chorowicz, J., Bellon, H., Richert, J.P., Mwanbene, J.T., Walgenwitz, F., 1988. East African Rift System: offset, age and tectonic significance of the Tanganyika-Rukwa-Malawi intracontinental transcurrent fault zone. Tectonophysics 148, 241–252.
Trauth, M.H., Maslin, M., Deino, A., Strecker, M.R., Bergner, A.G.N., Duhnforth, M., 2007. High- and low-latitude forcing of Plio-Pleistocene East African climate and human evolution. J. Hum. Evol. 53, 475–486.
Umazamo, A.M., Bellosi, E.S., Visconti, G., Melchor, R.N., 2012. Detecting allocyclic signals in volcaniclastic fluvial successions: facies, architecture and stacking pattern from the Cretaceous of central Patagonia, Argentina. J. S. Am. Earth Sci. 40, 94–115.
Vrba, E.S., 1988. Late Pliocene climatic events and hominid evolution. In: Grine, F.E. (Ed.), Evolutionary History of the "robust" Australopithecines. Aldine de Gruyter, New York, pp. 405–426.
Wescott, W.A., Krebs, W.N., Engelhardt, D.W., Cunningham, S.W., 1991. New biostratigraphic age dates from the Lake Rukwa Rift Basin in western Tanzania. Am. Assoc. Petroleum Geol. Bull. 75, 1255–1263.
Wheeler, W.H., Karson, J.A., 1994. Extension and subsidence adjacent to a "Weak" continental transform: an example from the Rukwa rift, East Africa. Geology 22, 625–628.
White, T.D., Suwa, G., 1987. Hominid footprints at Laetoli: facts and interpretations. Am. J. Phys. Anthrol. 72, 485–514.
WoldeGabriel, G., Heiken, G., White, T.D., Asfaw, B., Hart, W.K., Renne, P.R., 2000. Volcanism, tectonism, sedimentation, and the paleoanthropological record in the Ethiopian Rift System. In: McCoy, F.W., Heiken, G. (Eds.), Volcanic Hazards and Disasters in Human Antiquity: Boulder, Colorado. Geological Society of America Special Paper 345.
Zavala, C., Arcuri, M., Meglio, M.D., Gamero Diaz, H., Contreras, C., 2011. A genetic facies tract for the analysis of sustained hyperpycnal flow deposits. In: Slatt, R.M., Zavala, C. (Eds.), Sediment Transfer from Shelf to Deep Water—Revisiting the Delivery System. American Association of Petroleum Geologists, Studies in Geology, vol. 61, pp. 31–51.
Zavala, C., Ponce, J., Drittanti, D., Arcuri, M., Freije, H., Asensio, M., 2006. Ancient lacustrine hyperpycnites. A depositional model from a case study in the Rayoso Formation (Cretaceous) of west-central Argentina. J. Sediment. Res. 76, 41–59.